Republic of Iraq
Ministry of Higher Education & Scientific Research
University of Baghdad College of Education for Pure Science / Ibn Al-Haitham

Theoretical Comparison between HgCdTe and AlGaAs Heterostructure Quantum Well Laser Systems

A thesis

Submitted to the Council of the College of Education for Pure Science Ibn Al-Haitham, University of Baghdad in partial fulfillment of requirements for the degree of Master of Science in Physics

By

Wedian Kadhoum Abad Al-zubady

B.Sc. Physics (University of Baghdad) 2013

Supervised by

Dr. Ebtisam M-T. Salman

2016 A.C **1437 A.H**

بسم الله الرحمن الرحيم

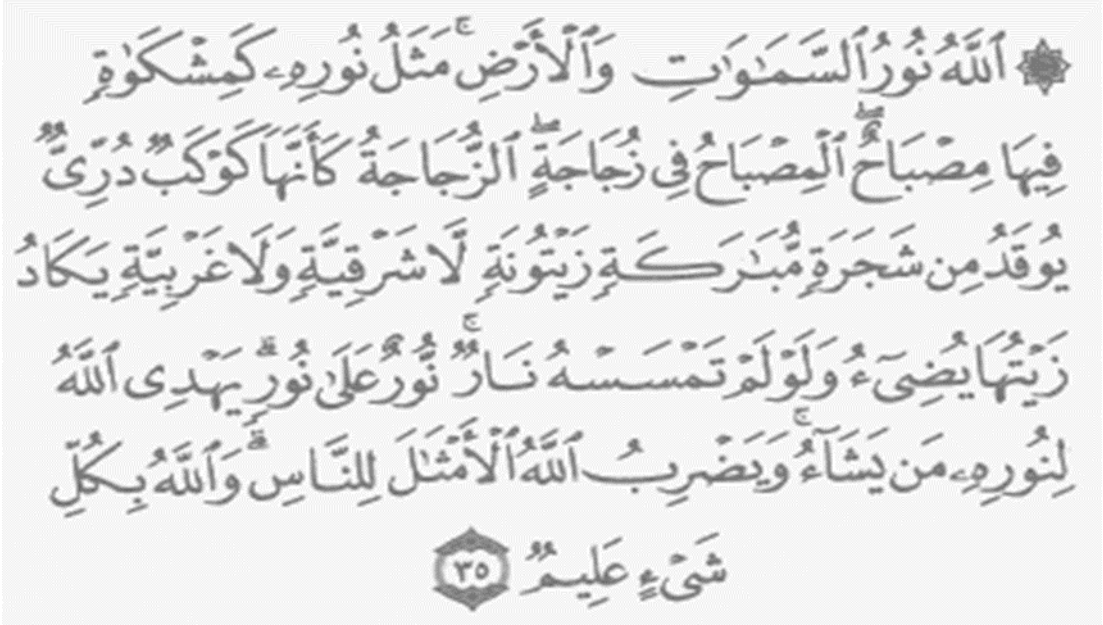

صدق الله العلي العظيم

سورة النور (اية 35)

This thesis is dedicated to:

The souls of Martyrs of Iraq, my dear parents, and my supervisor

Wedian

Acknowledgements

I would like to extend my thanks and appreciation to my supervisor of Dr.Ebtisam Mohammad T. For the proposed research topic and for her guidance and help in the duration of search, may God prolong her age to remain a beacon luminous in the way of science and scientists.

Also, I extend my thanks and gratitude to the College of Education, Ibn al-Haytham for pure sciences and the presidency of the Department of physics for their help and to all my professors, especially Dr. Ahlam.H.Jaffar AlMousawy who was the source of and guidance and tangible impact in that research until it shows the final image.

My thanks to all who gave me advice and guidance particularly by Dr. Mudhir Sh. Ahmed for giving me valuable guidance during the study.

Special thanks to Dr. Mahmood Radhi, I greatly appreciate his support and advice.

And also with pride and appreciation I would like to extend my thanks and gratitude to Mr. Abass Fadhil Al-Qaraghouli for encouraging me and help him overcome the difficulties during the study period.

I thank my friends who encouraged and help me during my research

Also thanks and appreciation to my parents who gave me care and encouragement, I ask God for their good health, happiness and success.

Wedian

Abstract

This work is description of theoretical comparison between two systems $Al_{0.3}Ga_{0.7}As/GaAs$ and $Hg_{0.2}Cd_{0.8}Te/Hg_{0.5}Cd_{0.5}Te$ for heterostructure quantum well laser. Where studied the effects of the variation parameters for this structure such as a well width, barrier width for Single and Multi-Quantum Well, on laser parameters such as optical confinement factor, threshold current, threshold current density, optical gain, output power and efficiency. In addition we studied the density of states for quantum well.

The optical confinement factor has the best value (0.308) for $Al_{0.3}Ga_{0.7}As/GaAs$ 3QWs at (W=21.5nm) and (0.0224) for $Hg_{0.2}Cd_{0.8}Te/Hg_{0.5}Cd_{0.5}Te$ 5QWs at (W=11.3nm). It introduced a significant improvement in MQW is much higher than SQW for two systems. The results showed that optical confinement factor of 3QW are much higher (by a factor 18) for $Al_{0.3}Ga_{0.7}As/GaAs$ and (by a factor 25) for $Hg_{0.2}Cd_{0.8}Te/Hg_{0.5}Cd_{0.5}Te$ 5QW, from optical confinement factor of SQW.

This investigated for improve the work of laser diode device through the effect of optical confinement factor on the gain, threshold current, output power and efficiency under forward bias in active region, where threshold current density $J_{th\ AlGaAs} = 5784\ A/cm^2$, $J_{th\ HgCdTe} = 1327\ A/cm^2$ with efficiency (89%for $Al_{0.3}Ga_{0.7}As/GaAs$ and 97% for $Hg_{0.2}Cd_{0.8}Te/Hg_{0.5}Cd_{0.5}Te$)

Chapter One

Literature Review

Chapter Two

Theoretical Investigation

Chapter Three

Results and Discussion

LIST OF FIGURES

List Of Abbreviation

DH	Double heterojunction
SH	Single heterojunction
2D-QW	2-Dimensional Quantum Well
1D-QWR	1-Dimensional Quantum Wire
0D-QD	0-Dimensional Quantum Dot
QW	Quantum well
SQW	Single quantum well
MQW	Multiple quantum well
DOS	Density of states
QCs	Quantum confined laser

LIST OF SYMPOLS

Symbols	Description	Unite
h	Planck's constant	J.sec
$\hbar$	Plank's constant divided by 2π	J.sec
q	Electron charge	C
d	Active region thickness	nm
R	Reflectivity	none
L	Cavity length	μm
E_g	Energy gap	eV
J_{th}	Threshold current density	A/cm^2
J	Current density	A/cm^2
I_{th}	Current	A
g_{th}	Threshold gain	cm^{-1}
g	Gain coefficient	cm^{-1}
T	Temperature	K
λ	Wavelength	nm
C	Normalized thickness of the active region	none
B	Barrier width	nm
W	Well width	nm
Γ^{SQW}	Single quantum well confinement factor	none
Γ^{MQW}	Multi quantum well confinement factor	none
N_w	Number of well	none
N_B	Number of barrier	none
α	Loss coefficient	cm^{-1}
K_B	Boltzmann's constant	J/K
E	Energy level	eV
x	Mole fraction	none
E_f	Fermi energy	eV
m^*	Carrier effective mass	kg
φ	Photon density	cm^{-3}
R_{re}	Recombination coefficient	cm^3/sec
υ	frequency	Hz

Symbols	Description	Unite
s	The velocity recombination	m/sec
τ	Lifetime of carrier	sec
τ_r	Radaitive lifetime	sec
τ_{nr}	Non Radaitive lifetime	sec
N_e	Electron concentration	cm^{-3}
P_e	Hole concentration	cm^{-3}
R_{eff}	Effective recombination coefficient	cm^3/sec
A	The area	cm^2
T_o	Characteristic temperature	K
d'	Average thickness	nm
γ_{rw}	Refractive index of active region	none
γ_{rc}	Refractive index of cladding	none
γ_r'	Average index refraction	none
V	Voltage	V
V_B	Built-in voltage	V
η_{int}	Internal efficiency	none
η_{ext}	External efficiency	none
η_{opt}	Optical efficiency	none
N_{ph}	Number of photon emitted	none
N_{inj}	Number of injection electron	none
ω	Angular frequency	Hz
P_{out}	Output power	W
η_s	Slope efficiency	none
P_{stim}	Power by stimulated emission	W
N_{th}	Threshold carrier concentration	cm^{-3}
A_{21}	Einstein coefficient for spontaneous	$cm^3.eV^{-2}$
B_{21}	Einstein coefficient for stimulated	$cm^3.eV^{-2}$
B_{12}	Einstein coefficient for absorption	$cm^3.eV^{-2}$
n_x, n_y, n_z	Quantum number	none
f_e, f_h	the Fermi Dirac distribution function for electron and hole	none

CHAPTER ONE

LITERATURE REVIEW

1.1 Introduction

Over the past decades there has been considerable interest in the physics of low- Dimension materials that exhibit highly anisotropic properties [1]. The evolution in technology has led to possibility producing materials with small dimensions lying between 1nm and 100 nm. These new materials called nanostructure materials [2,3]. It is a structure of intermediate size between molecules and bacterium [4]. In this structure properties become very size sensitive in these range. If one, two or three dimensions (1D, 2D, 3D) of a material downfall in the nanometer regimen, the materials may have astonishing properties which are very variance from the bulk materials [5].

For these dimensions, quantum mechanics are principles of implementation. One of the most effects of decreasing the size of materials to the nanometer range is the manifestation of quantization effects due to the confinement of the motion of electrons. This leads to discrete energy levels depending upon the size of the structure as it is known from the simple potential well treated in introductory quantum mechanics.

There are interests in active devices such as light emitting diodes (LED) especially laser diodes. These operations with wavelength rang (2-5μm), where these lasers represent a fundamental classification of electrical components have application with (industrial, medical, communication and optoelectronic device)[6,7].

In this chapter, semiconductor laser is explained with their structures, homojunction and heterojunction, Quantum well lasers, semiconductor laser materials, nanostructure semiconductor and their classification, density of states, and density of state of quantum well. It also includes the presentation of historical survey, and the aim of this study.

1.2 Semiconductor Laser

Semiconductor Laser diodes are main components in modern optical communications, medicine, and information processing. These types of devices were advanced and evolved constantly in the direction of size decrease and integration [8].

The semiconductor laser have several of advantage over the more conventional gas laser and solid state laser (small size, simple pumping, low cost, possible to modulation their injection current at high efficiencies and high frequency). In semiconductor laser diode characteristic parameters dependent on temperature as threshold current, quantum efficiency and lifetime [6,7,9].

Laser action is done by stimulated emission of recombination radiation from semiconductor p-n junction [10]. Optical gain is achieved through stimulated emission by electron-hole recombination which generates photons.

There are three major inter-band transition processes in the active region: absorption, spontaneous emission, and stimulated emission. In order to the optical gain occur, the probability of stimulated emission must be greater than probability of absorption. Optical gain is realization by electron-hole recombination which produces photons through stimulated emission. In the active region three main inter-band transition processes are existed: absorption, spontaneous emission, and stimulated emission. This happen when the quasi-Fermi energy discrete F_n-F_p exceeds the band-gap energy E_g and is referred to as population inversion. The mode arriving to threshold when the roundtrip gain is

controlling on the roundtrip loss for a resonant optical mode, and lasing action begins. The resonant cavity, which is commonly made by cleaving facets, provides the necessary feedback for the emission to be amplified, so that lasing oscillation can be sustained above threshold. Figure (1-1) shows the measured light-current-voltage [11]

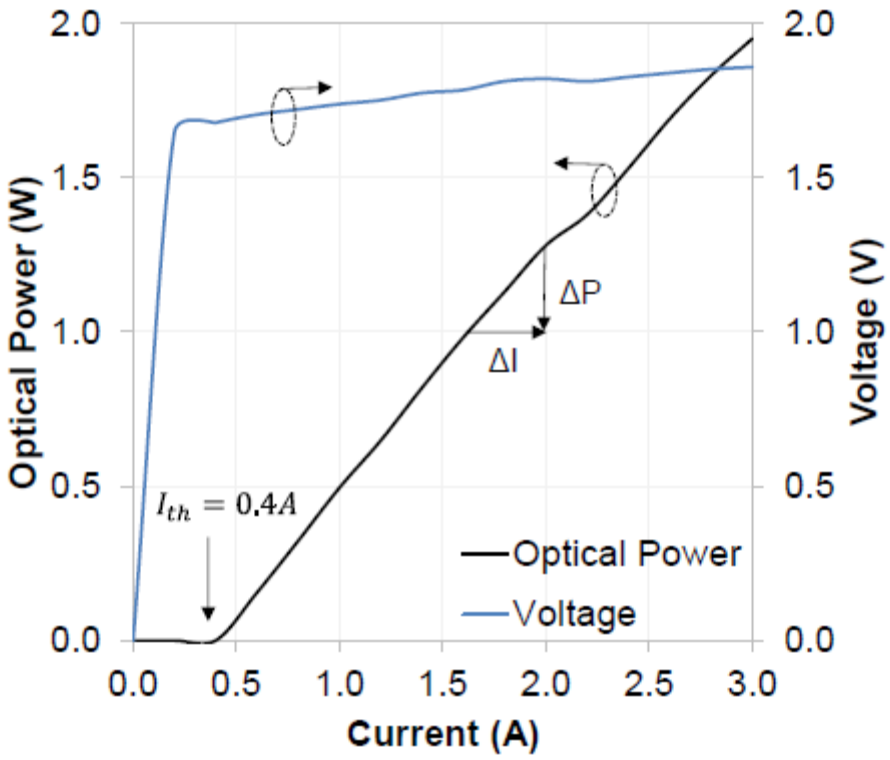

Fig. (1-1) Light-current-voltage characteristic of a typical semiconductor laser

1.2.1 The p-n junction

The pn junction is important to realize that the entire semiconductor is single-crystal material in which one region is doped with acceptor impurity atoms to form **p** region and the adjacent region is doped with donor atoms to form **n** region [5]. The interface separating the **n** and **p** region is referred to as the metallurgical junction.

1.2.1.1 The Junction at Zero Bias

In the equilibrium state the p-n junction without external connections to the semiconductor (zero bias), majority carrier of each type would diffuse across the junction, this process cannot continue indefinitely. As majority carrier- electrons in the n region will begin diffusing into the p region and majority carrier –holes in the p region will begin diffusing into the n region, electron and hole diffuse from area of high concentration toward area low concentration thus, electrons diffuse from the n region to the p region leaving behind positively charge (ionized donor atom). Similarly holes diffuse from the p region into the n region leaving behind negatively charge (ionized acceptor atom)[12]. As shown in Fig (1-2). The net positive and negative charges in the n and p regions induce an electric field in the region near the metallurgical junction, in direction from the positive to the negative charge, or from n to p region

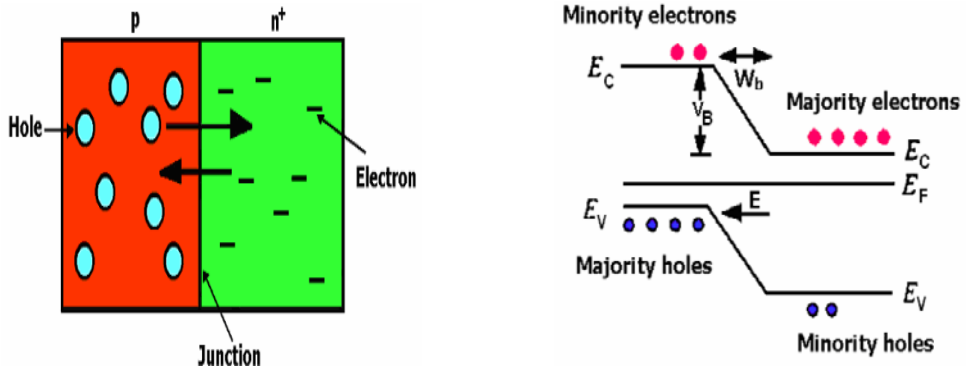

(a)

(b)

Fig. (1-2): (a) Majority carrier diffusion in pn-junction, (b) The energy band diagram of p-n junction showing the location of carriers under zero voltage bias

The narrow region on the both side of junction becomes lack of carrier of certain thickness is created at both side of the junction is called the depletion layer or space charge region as show in Fig (1- 3) [13, 14]

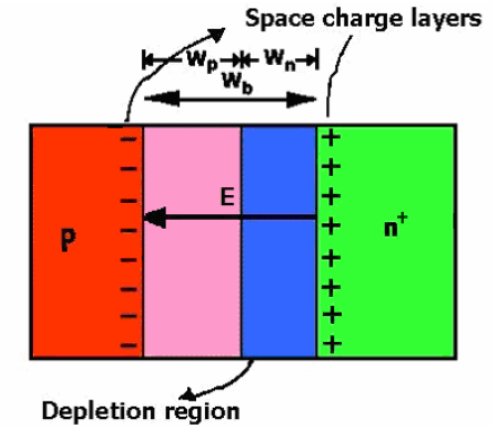

Fig. (1-3): p-n junction showing depletion region and electric field

1.2.1.2 The Junction under Forward Bias

If assume that p-n junction is forward biased by applying a positive voltage (V^+) to the p-region (holes motion right direction) and applying a negative voltage (V^-) to the n-region (electrons motion left direction), the effective voltage will across the junction is ($V_B - V$) where V_B the potential barrier. Thus the energy required by the majority carrier to overcome the potential barrier is less than zero voltage bias case (thickness depletion region is reduce), as result motion electrons and holes generation current in pn junction is called forward current and resistance of p-n junction is small, the presence of external bias voltage electric field is produced in a direction opposite to that of the built- in field. Fermi level become two Fermi levels in the depletion region, E_{fc} and E_{fv} represents a state of quasi-Fermi [13].

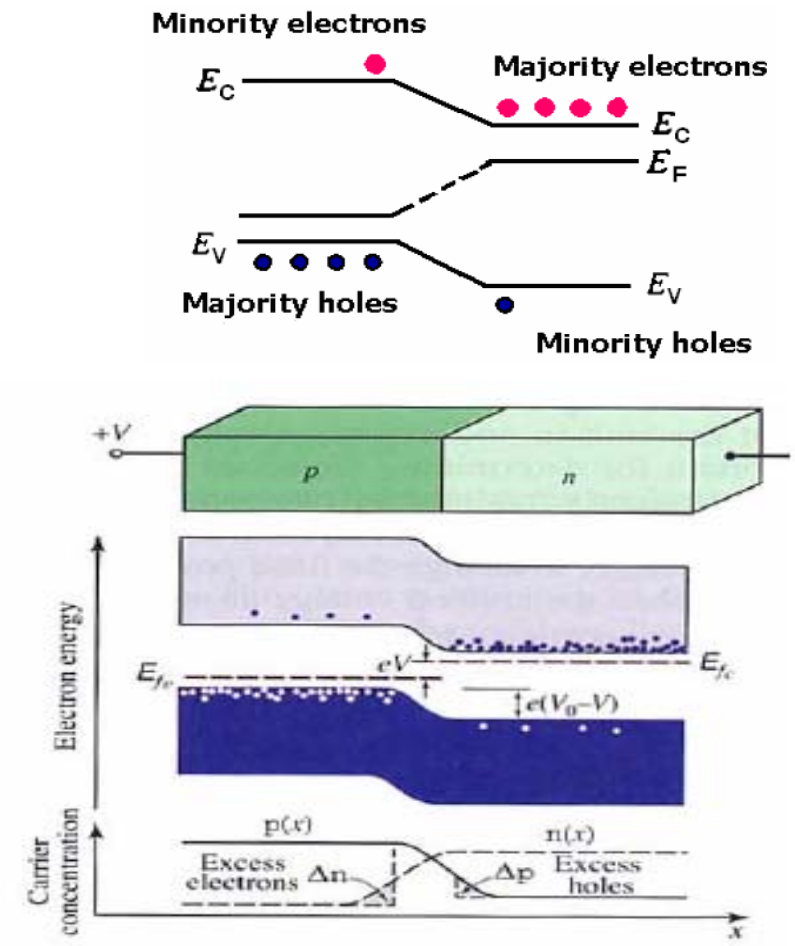

Fig.(1-4): The energy band diagram of p-n junction showing the location of carriers under forward bias.

1.3 Structures of Semiconductor Laser

1.3.1 Homostructure Lasers

The simple p-n junction is called homojunction, p type and n type material are same material (p, n regions have the same band-gap energies [15], the Fig. (1-5) shows p,n regions make from material GaAs as basic structure, a pair of parallel planes is cleaved where act as reflecting mirrors for resonator[16,10]

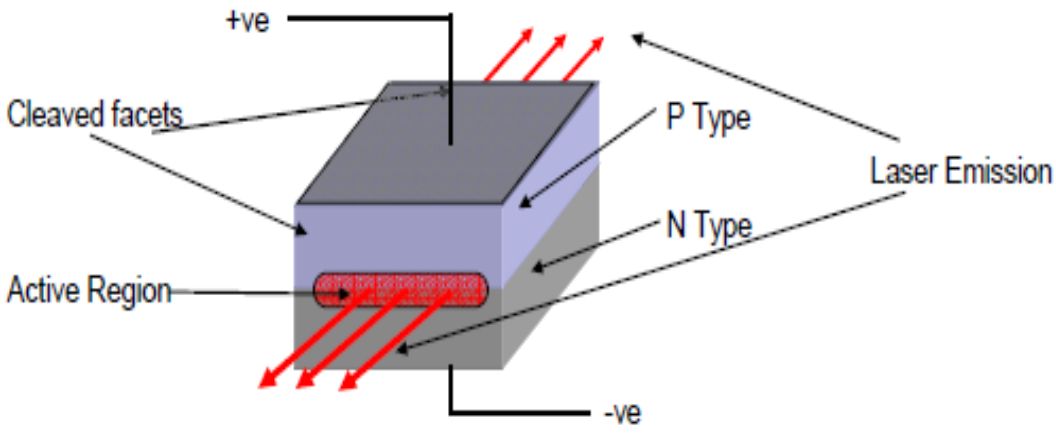

Fig (1-5): A schematic illustration of GaAs homojunction laser [16].

The difference in doping provided a small step in the index of refraction, the fig. (1-6) shows a homostructure with the refraction index of material is varying as one goes through it .The tended to supply some confinement of light in the layer of the junction, on account of total internal reflection. But, the step in the index of refraction is tiny and the confinement exceedingly poor. The prevalence of light out of active layer were large cause cavity losses, so that the actively current had to be high, and these devices were subject to damage and short-lived [12] to minimize the loss prefers to use heterostructure

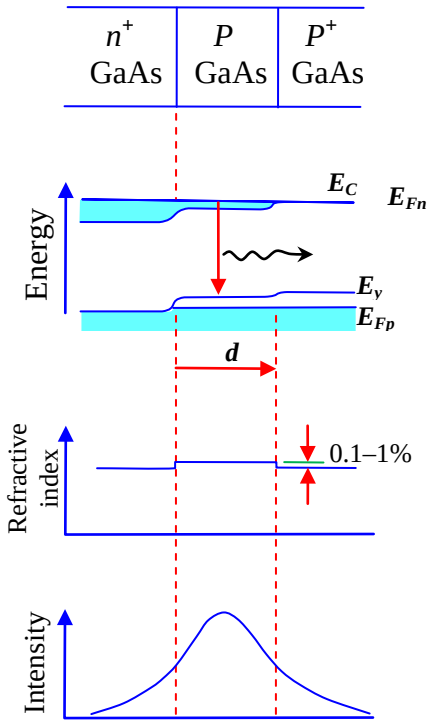

Fig.(1-6):homojunction and index of refraction in the GaAs system[10]

1.3.2 Heterostructure Lasers

A p-n junction is called heterojunction, when p type and n type material are difference material (p, n regions have different band-gap energies [15], the Fig. (1-7) shows p region make from material GaAs as basic structure, but n region make from material AlGaAs, or p-AlGaAs.

There are two types of heterostructure laser, Single heterojunction (SH) consists of p-type and n-type different semiconductor materials and band gap energy. In double heterojunction laser, a low band-gap material which is sandwiched between two high band gap material [17], one commonly used pair of material is GaAs with $Al_xGa_{1-x}As$ each of the junction between different band gap material is called a heterojunction, hence the name double heterojunction (DH) laser. The advantage of a double heterojunction laser over a homojunction laser is

the region where free electrons and holes exist simultaneously are confined to the active region when electrons injected n-type region and holes injected in p-type region, this carrier confined in active region and cannot escape because the carrier need to high energy, thus electron and hole forced to recombine in the active layer, therefore reducing the leakage current and increasing efficiency of the laser device [17, 18].

Heterostructures in generic have many uses. They can be used for advanced electronic devices (e.g., heterojunction bipolar transistors and resonant tunneling devices), optical components (e.g., waveguides, mirrors), and optoelectronic devices (e.g., laser diodes, photodetectors, quantum well and superlattice optical). Although heterostructures may be useful in electronics, they are conclusive in many optoelectronic devices (e.g., lasers). Perhaps their most important technological aspect may be that they can be used for all of these electronic, optical and optoelectronic purposes [19]

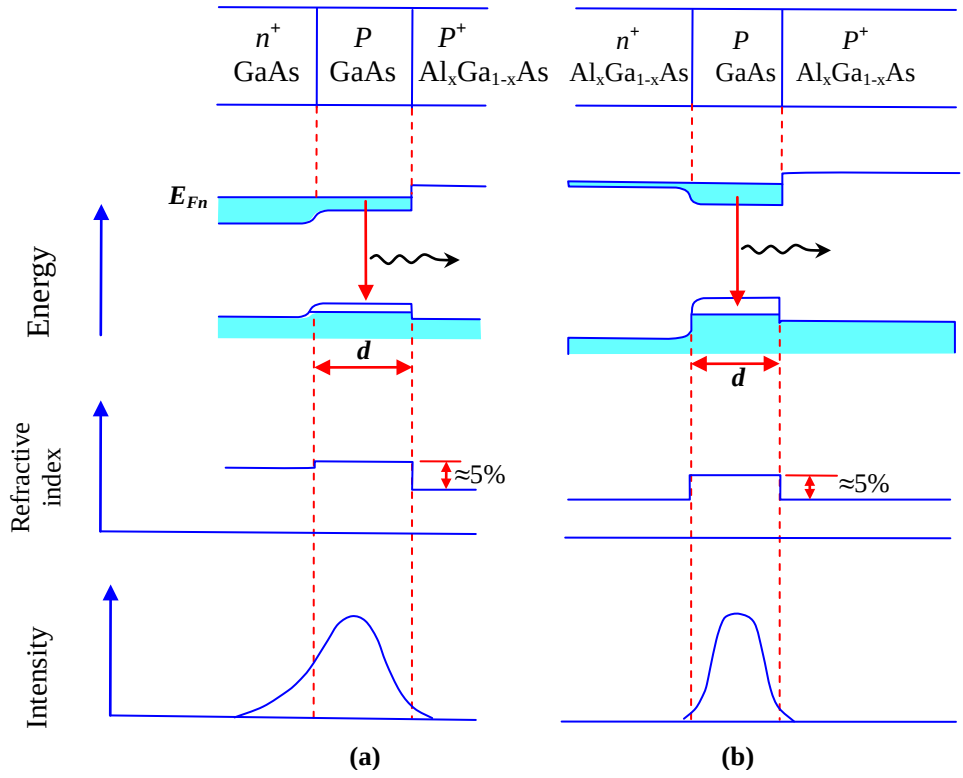

Fig.(1-7). (a): Single heterostructure. (b): Double heterostructure[10]

1.3.3 Quantum well lasers

A quantum well (QW) laser is a particular type of heterostructure in which the active region contain a thin layer of a narrow gap semiconductor material "well" existent between two wide band-gap semiconductor material "cladding" [20]. The layers separating the active regions are called barrier layer as shown in fig. (1-8).

The QW laser improves the performance of laser diodes in terms of low threshold current and narrow emission band. In this structure the emitted wavelength depends on nanostructure dimension (quantum size effect) [8].

The electrons in the conduction band and holes in the valence band of well layer, lower energy that called "potential well". In this layer the

electrons and holes are confined, the quantum confinement occurs with a highly-concentrated density of states [19].

In this structure, electron and hole are move in to the allowed states correspond to standing waves in the direction orthogonal to the layers. Because only particular waves are standing waves, this system is quantized, hence the name "quantum well".

The active region of a double-heterostructure laser (DH) is thin layer with width (*W*) in order of the De Broglie wavelength *($\lambda = h/p$)*, 2D quantization occurs, in order that a series of separate energy levels given by the confined-state energies of a finite square well. These devices are called quantum-well laser [10]. The wavelength of the laser light which emitted by a quantum well laser is determined by the well width of the active region Instead of simply just the band-gap of the semiconductor material from which it is constructed [21]. The quantum well laser divide two type: one quantum well layer (active region) is called *single quantum well* (SQW) Laser, while the active region consists from more than one quantum well layer separate alternating with barrier layers is called as *multi-quantum well* (MQW) laser.

MQW is a structure consisting of an alternating pattern of narrow and high band-gap materials [5]

Multi-quantum wells improve the efficiency further [17]. Existing two type of multi-quantum well (i) Multi quantum well laser consists of several active layers, (ii) Modified Multi quantum well laser when the band-gap energy of the barrier layer vary from the cladding layer in a Multi-quantum well device as shown in fig. (1-8) [5]

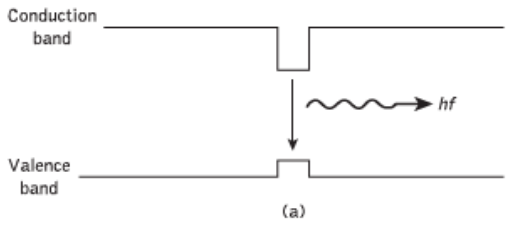

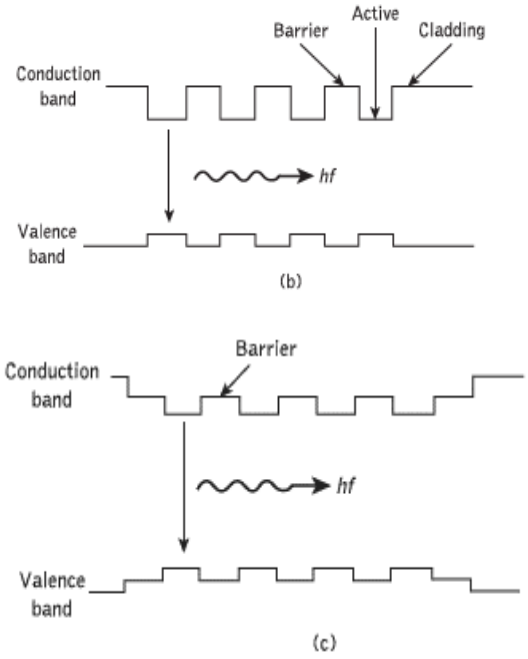

Fig. (1-8) types of Quantum Well laser (a: Single QW, b: Multi-QW and c: Modified QW)

The most important principal parameters for a semiconductor laser are population inversion and quantum efficiency. The population inversion is more amenable to optimization by adjustments in layer thicknesses and material compositions [9]. The quantum well is a result of the evolution in the epitaxial layer growth technology. The important Characteristic of the quantum well structure is the large improvement of the lasing action due to the variation of the energy level distribution of the semiconductor material when its thickness (d) is decreasing below 20 nm [16]. The high concentration of charge carriers in the narrow bar of the active material reduces the threshold current required to initiate lasing. The high band-gap layers on either side of the active layers carry out confinement of charge carriers to the active materials as well as confinement of the laser output to a narrow width. The optical confinement in the optical mods obtained in Multi-quantum well best of Single quantum well thus threshold current density is low [5].

1.4 Semiconductor Laser Materials

There are many semiconductor materials with different electrical and optical properties in order to obtained appropriate laser. The major parameter which distinguishing these materials is the width of band gap. All semiconductor laser materials have direct band gaps [10]. This is expected because the momentum is conserved and no phonon is expected, this mean the electron in low conduction band (C_B) have same momentum at the high of the valence band (V_B) as show in Fig. (1-9)[22, 23]. The radiative transition in this material is a first-order process (no phonon involves) and the quantum efficiency is expected to be much higher than that for an indirect- band-gap semiconductor, where a phonon is involved. This material used in active layer of laser diode such as: GaAs and HgCdTe

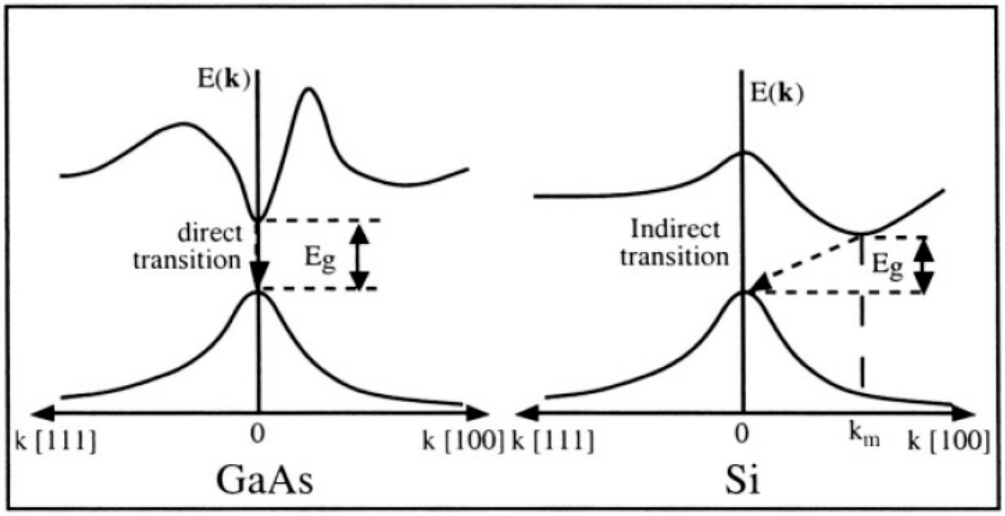

Fig.(1-9): show the direct band gap semiconductor (left) and indirect band gap semiconductor (right) [22]

1.4.1 GaAs

Gallium arsenide is the earliest material used for high-efficiency LEDs, the first material to emit laser radiation and its related III- V

compound alloy are the most widely studied and developed. GaAs have a zinc-blend structure, and used in microwave and photonic applications, have width of energy band gap is (1.42 eV) [10, 24]. The transition type in GaAs is direct band gap which the energy and momentum conservation. In GaAs emitting photon with a wavelength corresponds to near-infrared, almost visible light.

The $Al_xGa_{1-x}As$ is the ternary compound system including a wide range of wavelength from red to infrared [10]. Band gap of $Al_xGa_{1-x}As$ different with composition

$$E_g(x) = 1.424 + 1.266x + 0.26x^2 \qquad (1\text{-}1)$$

For $x < 0.45$ the band gap is direct [25], the refractive index of AlGaAs depended on mole fraction [26].

$$\gamma_r = 3.59 - 0.71x + 0.091x^2 \qquad (1\text{-}2)$$

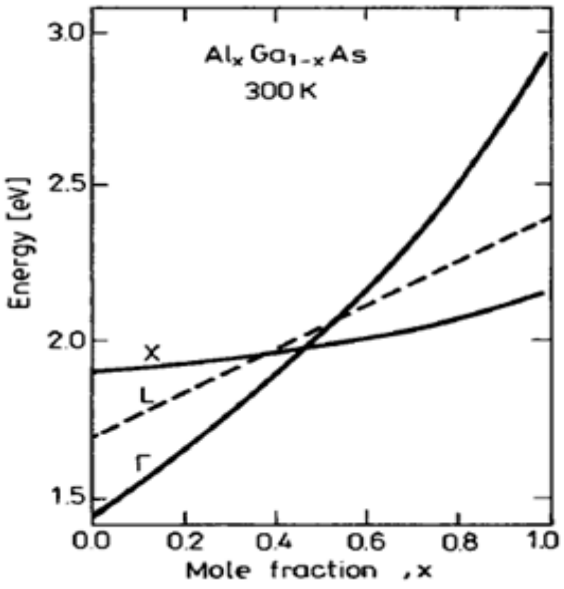

Fig.(1-10) The energy gap of AlGaAs as function of Al composition (*x*)

1.4.2 HgCdTe

The material Mercury Cadmium Telluride ($Hg_{1-x}Cd_xTe$) is a ternary alloy with direct band gap [27], zinc-blend crystal structure and II-VI compounds semiconductor, the band gap for $Hg_{1-x}Cd_xTe$ is given by [28]:

$$E_g = -0.302 + 1.93x - 0.81x^2 + 0.832x^3 + 5.35 * 10^{-4}(1 - 2x)T \quad (1\text{-}3)$$

Where E_g measurement in unit eV,T:the temperature in unit Kelvin.

Mercury Cadmium Telluride $(Hg_{1-x}Cd_xTe)$ is a good candidate material for lasers in IR wavelength range [27, 29]. Energy band gap depended on the composition and temperature [30], but $Hg_{0.5}Cd_{0.5}Te$ has energy gap independence on temperature, it is a good material for cooling because of high electrical conductivity and low thermal conductivity at 300 *K*, where cooling is very important of laser device. Many studies have been carried out on this topic but performed little research on Mercury Cadmium Telluride (HgCdTe). The electrical and optical properties determined by the energy gap structure [31]. In $Hg_{1-x}Cd_xTe$ intrinsic carrier concentration (N_i) calculated through the equation:

$$N_i = (5.585 - 3.83x + 0.001364xT) * 10^{14} E_g^{\frac{3}{4}} T^{\frac{3}{2}} \quad (1\text{-}4)$$

Which all parameters of $Hg_{1-x}Cd_xTe$ are very sensitive to cadmium composition (*x*) and temperature [30].

The refractive index γ_r for material $Hg_{1-x}Cd_xTe$ can be calculated from the following formula [32]

$$\gamma_r = 4.427 - 3.617x + 2.055x^2 \quad (1\text{-}5)$$

1.5 Semiconductor Nanostructure

Reducing dimensionality of the active region improves significantly the performance of semiconductor lasers [33, 34]. The semiconductor nanostructures have been investigated now for more than 30 years. They have found a high number of applications in the technology, just to remind few of them: lasers, light emitting diodes, light detectors or transistors. This number is increasing and these structures are for the time being considered to be even more show for future applications e.g. for quantum computing. This is one of the reasons why after this a long time the amount of research performed on this field does not decrease but increases further [35]. Nanostructure results from new fabrication technologies where shape control, size control and uniformity can be maintained with the precision of nanometer (nm) scale [2, 36].

One of the most direct effects of reducing the size of materials to the nanometer range is the appearance of quantization effects due to the confinement of the movement of electrons. This leads to discrete energy levels depending on the size of the structure as it is known from the simple potential well treated in introductory quantum mechanics.
Semiconductor nanostructures are classification according their chemical composition or dimensionality. The most common semiconductor nanostructure a classified accords the dimensionality [2, 37].

Let us assume that we have an electron in box of dimensions L_x, L_y, L_z. then how many dimensions on the nanoscale (smaller than the characteristic length L_C) [37,38]. Characteristic length is the description of the behavior of electron in semiconductor material, such as de Brogli wavelength, mean free path, diffusion length[38,39], or Bohr radius)[2,40], these lengths correspond to physical properties of

electron which are size dependent. We can have the following situation; If

i) All dimensions larger than L_C $(L_x, L_y, L_z > L_C)$ The electron behaves as in regular 3-D bulk semiconductor. There are three degree-of freedom direction which does not confined direction [37].

ii) Only one dimension smaller than L_C and another two dimensions larger than L_C, this system is called a quantum well (QW). The motion of electrons in QW is restricted in one dimension and free motion in another two dimensions, such as$(L_y, L_z > L_C > L_x)$. This situation acts as a 2-D semiconductor perpendicular to the x-axis [2, 38, 40].

iii) Two dimensions smaller than L_C and another dimension larger than L_C, this system is called a quantum wire (QWR). The motion of electrons in QWR is restricted in two dimensions and free motion in another one dimension, such as $(L_z > L_C > L_x, L_y)$. This corresponds to a 1-D semiconductor or quantum wires, located along the z-axis. There is one degree-of freedom direction.

iv) All dimensions smaller than L_C $(L_C > L_x, L_y, L_z)$ In this case the charge carriers confined in three directions the structure is called a 0-D semiconductor or quantum dot (QD).

The characteristic lengths which vary widely from material to material and also with temperature, applied field, impurity concentration, ect[4].

1.6 Density of states

One important advantage of nano-scale semiconductor materials for laser applications originates from a noticeable increase of the density of the state for electron and holes with the reduction of dimensions [41].

The density of state(DOS) function at give value E of energy is defined such that $\rho(E)\Delta E$ is equal to the number of state in interval energy ΔE around E [36], the DOS is essential for determining the carrier concentration and energy distribution of carriers with in a semiconductor[42].

We can defined DOS (is the material property which quantifies the number of the carriers that are permitted to occupy a given energy state of semiconductor [41], or the number of state per unit volume per unit energy [43]. The density of state for bulk is [44].

$$\rho_{bulk}(E) = \frac{1}{2\pi^2}\left(\frac{2m^*}{\hbar^2}\right)^{3/2}\sqrt{E} \qquad (1\text{-}6)$$

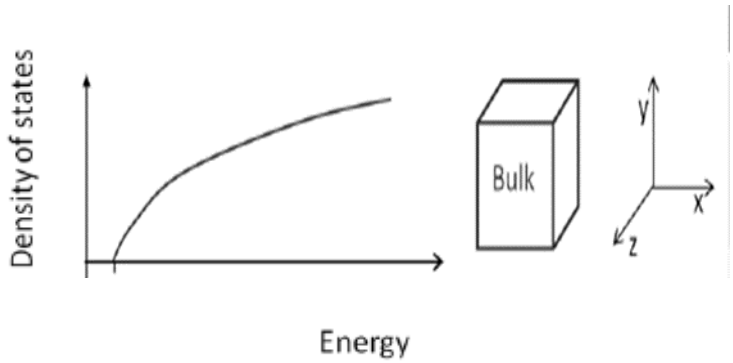

Fig(1-11) density of state for electron in bulk semiconductor

Density of state in eq.(1-6) depending on square root energy [45]. In the bulk semiconductor conduction band and valence band are continuous because there are no quantum effect while the quantum effects in

quantum well occurring in only one dimension and energy bands are discrete instead of the continuous energy bands [25], fig.(1-12).

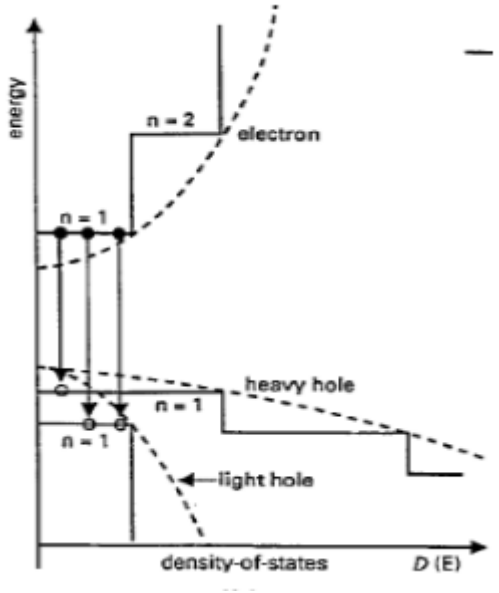

Fig.(1-12) density of states for quantum well (solid line) and bulk semiconductor (dotted line)

1.6.1 Quantum Well

The electrons and holes are confined in one direction and have two degrees of freedom in other two direction [44], density of states in 2-D system is restricted to the k_x, k_yplane shown in fig.(1-13), the total number of states per unit cross-sectional area is given by the area in k-space divided by the area of the unite cell in k-space and divided by the area in real space[46]

$$N^{2D} = 2\pi K^2 \frac{1}{(\frac{2\pi}{L})^2}\frac{1}{L^2} = \frac{2\pi K^2}{(2\pi)^2} \qquad (1\text{-}7)$$

Where factor 2 is the spin degeneracy of electron, $L^2$is the real space area, and $(2\pi/L)^2$ is the two- dimensional primitive unit cell in k-space. The DOS for QW can be given by:

$$\rho(E) = \frac{dN^{2D}}{dE} = \frac{dN^{2D}}{dk}\frac{dK}{dE} \quad (1\text{-}8)$$

$$\rho(E) = \left(\frac{k}{\pi}\right)\left(\frac{2m^*}{\hbar^2}\right)^{\frac{1}{2}} \frac{1}{2\sqrt{E}} = \frac{m^*}{\pi\hbar^2} \quad (1\text{-}9)$$

m^* is the effective mass, E is the energy and defined by:

$$E = \frac{\hbar^2 k^2}{2m^*} \quad (1\text{-}10)$$

Density of states independent of energy. If there is more than one confined state in quantum well system, the density of state is given by the following:

$$\rho(E) = \sum_{j=1}^{n} \frac{m^*}{\pi\hbar^2} Y(E - E_i) \quad (1\text{-}11)$$

Where n is the total of confined sub-bands below a particular energy and Y is a step function defined as the following

$$Y(E - E_i) = \begin{cases} 1 \; for \; E > E_i \\ 0 \; for \; E < E_i \end{cases} \quad (1\text{-}12)$$

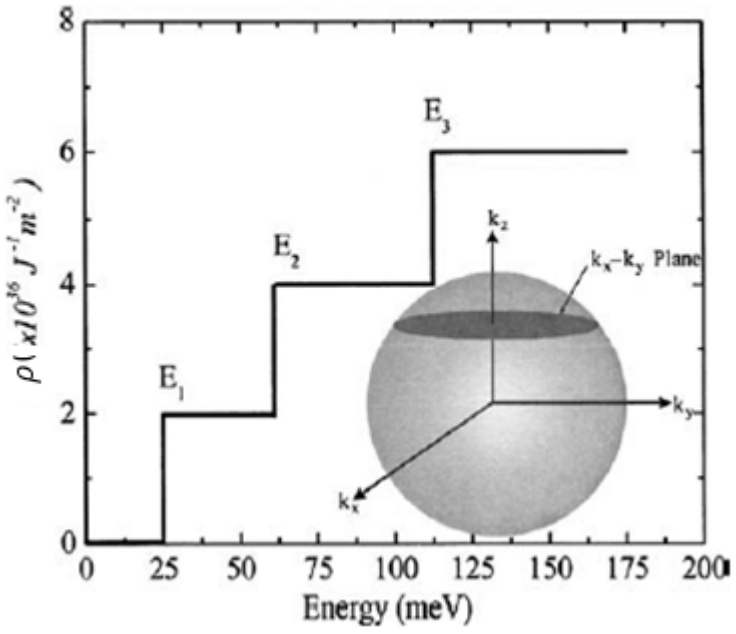

Fig.(1-13) Electron in two dimension

1.6.2 Quantum-Wire

The electrons and holes are confined in two direction and have one degree of freedom in structure [44]. In Q-wire confinement in two dimensional (k_y, k_z) in k-space and one direction is free k_x, the total number of states N can be obtained by dividing the total length (L) of Q-wire (2k) (due to the electron moment fill state a long a line such as Fig.(1-14) by the primitive unit cell and then dividing by the length in the real space[46].

$$N^{1D} = 2\frac{2k}{(\frac{2\pi}{L})}\frac{1}{L} = \frac{2k}{\pi} \qquad (1\text{-}13)$$

Where N^{1D} is the total number of states, 2 is the spin degeneracy of electron.

Then the DOS for QWR is given by:

$$\boldsymbol{\rho(E) = (\frac{2m^*}{\hbar^2})^{1/2}\frac{1}{\pi\sqrt{E}}} \qquad (1\text{-}14)$$

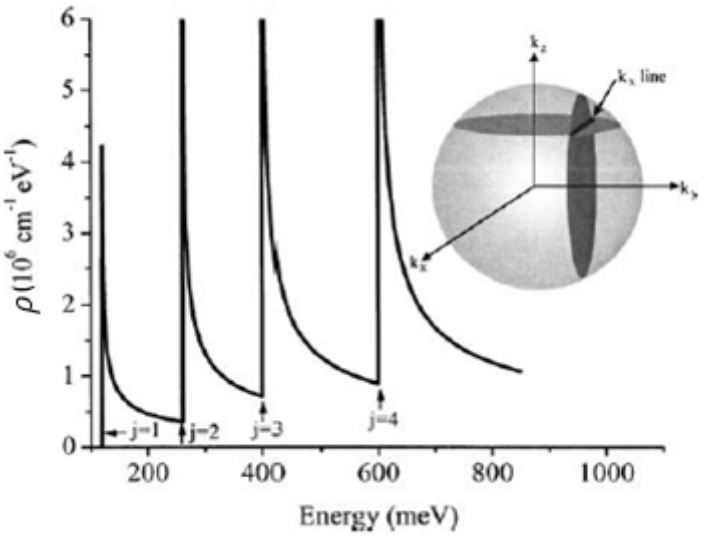

Fig.(1-14) Electron in one dimension

1.6.3 Quantum-Dot

Quantum dot is one types of semiconductor nanostructure the electron are confined in all three dimensions, where the density of state is a series of delta functions given by:

$$\rho(E) = 2\delta(E - E_{n_x,n_y,n_z}) \qquad (1\text{-}15)$$

Where E_{n_x,n_y,n_z} are the confined energies of the carrier and the factor 2 accounts for spin degeneracy [45]. The fig. (1-15) illustrated the density of state for Q-dot

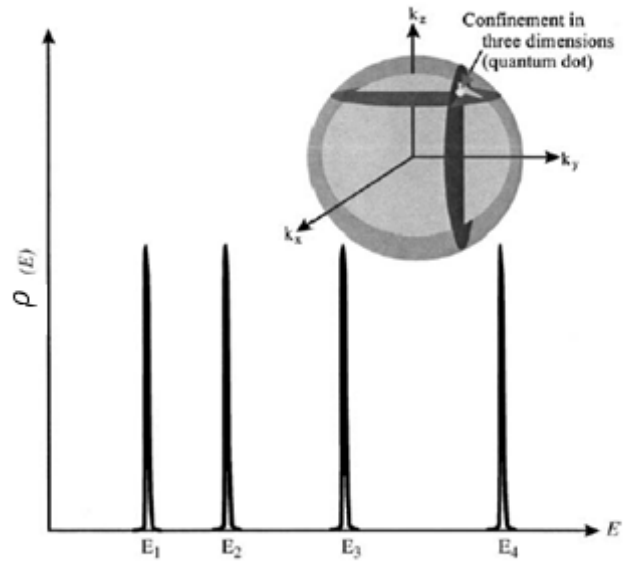

Fig.(1- 15) Electron in zero dimension

The DOS represented by the number of confined states divided by the energy interval, if the energy interval is approaching zero then the density of state is simply a series of δ-function centered on the confined energy levels $(E_1, E_2, E_3, \ldots.)$ the energy levels are entirely discrete and are given by [46]

$$E_{n_x,n_y,n_z} = \frac{\pi^2\hbar^2}{2m^*}\left(\frac{n_x^2}{L_x^2} + \frac{n_y^2}{L_y^2} + \frac{n_z^2}{L_z^2}\right) \qquad (1\text{-}16)$$

1.7 Historical Survey

The development of semiconductor through the year in 1970 successful heterostructure laser operating continuously at room temperature and threshold current density as low as $1.6 * 10^3 A/cm^2$, the quantum well laser had been demonstrated in 1975 and 1977[47],

In the beginning of 1980 quantum well structure in the active region was invented to achieve more efficiency of laser [48]. Y.Arakawa, A.Yariv, discuss the basic properties of quantum well laser with

emphasis on its dynamic and spectral properties and gain characteristics in 1986[49].

In 1991 Y.Jiang, et al calculated carrier lifetime and threshold current in HgCdTe double heterostructure and multi-quantum well lasers [50]. Anatoli S.polkovnikov and Georgy.G.Zegrya in year 1998 have Auger recombination in semiconductor quantum well [51]. In the same year Alex T.H. Li, et al found a theoretical model is presented for investigating AlGaAs/GaAs Q-well vertical cavity waveguides defined by impurity –induced disordering [52]

In September 2002 by Manish Jain interested the quantum well about 1550 nm, they studied broadening the gain spectrum of MQW laser by including multiple width QW in active region and study in the advantages obtained experimentally over conventional identical width quantum well laser [53].

In 2004" A. Stintz, et al compare the spectral dependence of modal gain and line width enhancement factor for two types of laser a convential GaInAs QW laser and a laser of same design and GaInAs QW ,but with InAs Q dot in the well forming the active media [54]. In February 2005 N. Tansu and Luke J. Mawst, have explain the behavior of the current/carrier injection efficiencies in the 1200 nm emitting InGaAs QW and 1300 nm emitting InGaAsN QW laser[55].

In 2008 Jonathan M. Buset studied investigation in to use of polarized light to manipulation the properties of a GaAs/AlGaAs QW laser [56]. Also in the same year H. Zhao,et al. Nelson Tansu have analyze the optical gain properties of strain-compensate InGaN QW employing tensile barriers of AlGaN emitting in the 420-500 nm regimes [57].

In April 2010 S.A. Sayid et al, They have investigated threshold current and different quantum efficiency as the function temperature in InGaAlAs/InP MQW buried heterostructure (BH) laser [58]. A. Asgari, S. Dashti, Optimization of optical gain in $Al_xGa_{1-x}N/GaN/Al_xGa_{1-x}N$ Strained quantum well laser, they have analyze the optical gain properties and the effect of temperature, carrier concentration, quantum well width and barrier width [59]

In 2011, J. W. Ferguson, P. B. and P. M. Smowton , they have Optical Gain in GaInNAs and GaInNAsSb Quantum Wells [60]. In 2013 Michael Wootten, report on the performance of GaInAsSb/AlGaAsSb QW heterostructure operation in the 2-2.5μm wavelength rang at room temperature using simple straight ridge waveguides with angle facets [61].

Tawsif Ibne Alam, Md. Abd Al- Rahim,Rinku Basak in 2013 studied the effect of variation of QW number on the performance of designed 635 nmGaInP(AlGa)InP multi-quantum well separate confinement heterostructure red laser are presented considering the effects of quantum well number variation[62].

1.8Aim of this study

A comparative study between HgCdTe and AlGaAs Quantum well semiconductor laser of hand the effect of:

1. The single and multi -quantum well on the value of optical confinement factor
2. The cavity length on the gain coefficient.
3. The structure parameter such as well width, barrier width on the optical confinement factor, threshold current density, internal and external efficiency, and output power.

CHAPTUR TWO

THEORETICAL INVESTIGATION

2.1 Introduction

This chapter reviews the expressions which are needed for theoretical calculations of the important parameters used in this work. Potential well The optical transition, Recombination processes and carrier lifetime The optical confinement factor, the density of states, threshold current density, the optical gain, and output power for the quantum wells laser have been investigated.

2.2 The Electron in Potential Well

The study energy spectrum of an electron confined in 1D quantum well, we assume that carrier exists in square potential well as shown in Fig. (2-1) where the potential energy of the electron depending on only one coordinates and can be written as [63]

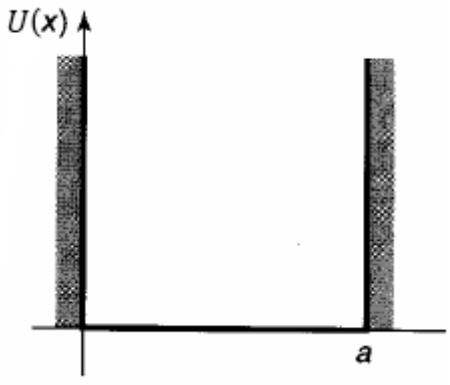

Fig.(2-1) the potential well

The infinite square well potential is given by:

$$U(x,y,z) = \begin{cases} o & inside\ the\ well \\ \infty & outside\ the\ well \end{cases}$$

The potential $U(x,y,z)$ is not periodic when potential well is cube with a side (L) , the Schrodinger equation is gave by

$$-\frac{\hbar^2}{2m^*}\nabla^2\psi(x,y,z)+U(x,y,z)\psi(x,y,z)=E\psi(x,y,z) \qquad (2\text{-}1)$$

Where

$$\psi(x,y,z)=\psi_1(x)\psi_2(y)\psi_3(z) \qquad (2\text{-}2)$$

$$U(r)=U_1(x)+U_2(y)+U_3(z) \qquad (2\text{-}3)$$

$$E=E_1+E_2+E_3 \qquad (2\text{-}4)$$

By substitute Eq. (2-2),(2-3) and (2-4) in eq. (2-1) we can obtain:

$$-\frac{\hbar^2}{2m^*}\left[\frac{d^2\psi_1(x)}{dx^2}+\frac{d^2\psi_2(y)}{dy^2}+\frac{d^2\psi_3(z)}{dz^2}\right]+U_1(x)\psi_1(x)+U_2(y)\psi_2(y)+U_3(z)\psi_3(z)=$$

$$(E_1+E_2+E_3)\psi_1(x)\,\psi_2(y)\,\psi_3(z) \qquad (2\text{-}5)$$

The full wave function [64]:

$$\boldsymbol{\psi_{x,y,z}=\psi_1(x)\psi_2(y)\psi_3(z)=\sqrt{\frac{8}{V}}\,\sin\left(\frac{\pi n_x}{L_x}\right)\sin\left(\frac{\pi n_y}{L_y}\right)\sin\left(\frac{\pi n_z}{L_z}\right)} \qquad (2\text{-}6)$$

Where $V=L_xL_yL_z$ is the volume of quantum well

2.3 Recombination processes and carrier lifetime

The carriers recombination lifetime is one of the most important parameters as it both characterizes the semiconductor materials and it strongly influences devices properties [65]. When the injected of electric current through a semiconductor laser that ideally generates single photon for each injected electron-hole pair. But there are other processes are often increasing that the threshold current, and thus lead to a deterioration of the performance of the device. The total current in a semiconductor at threshold, is obtained by different terms depending on carrier

concentration through each recombination via defects, radiative recombination, non-radiative Auger recombination and carrier leakage[66].

There are two types of recombination, the radiative recombination and non-radiative recombination. The radiative recombination occurring when the carriers in conduction band (electrons) and valence band (holes) recombine which radiative light will be emitted from this process (photon emitting). The radiative include (a)- Spontaneous emission (b)-Stimulated emission (c)- Gain or absorption, While the non radiative recombination occurring when the carriers in conduction and valence band recombine non radiative which no light will be emitting from process but the emitting be in form heat and needed to increasing current in order action lasing, non radiative divided to (a)- Auger recombination (b)-Surface recombination (c) Recombination at defects [44].

The parameter in recombination is carrier lifetime defined as the time that carriers exists in active region before recombination , the total lifetime in process recombination can be written as [67]

$$\frac{1}{\tau} = \frac{1}{\tau_r} + \frac{1}{\tau_{nr}} \qquad (2\text{-}7)$$

τ_r, τ_{nr} are the lifetime of radiative and non radiative respectively, in the device the heterostructure the lifetime change with recombination region width (d) and the velocity recombination (S) as in equation [68]

$$\frac{1}{\tau} = \frac{1}{\tau_r} + \frac{1}{\tau_{nr}} + \frac{2S}{d} \qquad (2\text{-}8)$$

The carrier lifetime depending on the injection carriers (concentration)[5].

$$\tau_r = [B_{re}(N_o + p_o)]^{-1} \qquad (2\text{-}9)$$

Where τ_r, B_{re}, N_o, p_o are the radiative lifetime, the recombination coefficient electron and hole concentration respectively. The radiative lifetime reduce with increasing the injection current density as the following equation [69]

$$\tau_r = \left[\frac{dq\,(N_o+p_o)}{J^2}\right]\left\{\left[1+\frac{4J}{qB_{re}d(N_o+p_o)^2}\right]^{\frac{1}{2}}-1\right\} \qquad (2\text{-}10)$$

2.4 The optical transition

The transitions of electrons from high energy states to low energy states in semiconductors are specified recombination of the electrons and the holes. In the recombination of the electrons and the holes, the recombination divided into two types radiative recombination and nonradiative recombination. The photons emit from the radiative recombination, and the energies of the photons correspond to a variation in the energies between the initial and final energy states related to the transitions. In disparity, in the nonradiave recombinations, the phonons are emitted to crystal lattices or the electrons are trapped in the defects, and the transition energy is transformed into forms other than light. The Auger processes are also classified as nonradiative recombination. To obtain high efficiency semiconductor light emitting devices, we have to decreasing the nonradiative recombination. However, to enhance modulation characteristics, the nonradiative recombination centers may be intentionally induced in the active layers, because they decrease the carrier lifetimes (see Sect. 2.3)[64]. In a HgCdTe quantum well (QW) the Auger recombination rate is shown to be significantly smaller than that in bulk material [50]. As well known, the quantum effect in quantum well occurring in only one dimension and energy bands are discrete in both

conduction and valance band instead of the continuous energy bands in bulk[70]

There are two types of the optical transition, inter-band transition occur between the conduction and valance bands included two carriers (electrons and holes) the energy of the transition is the band-gap energy plus the confinement energies of the electrons and holes, The allowed transition in this type is ($\Delta n=0$). But , the other type is the inter-subband transition take place inside the conduction band or the valence band between two subbands are called inter-sub band transition such as quantum well and quantum wire, in the quantum dot transition happen between discrete energy levels and the allowed transition is ($\Delta n=1$)[71] as shown in fig.(2-2)

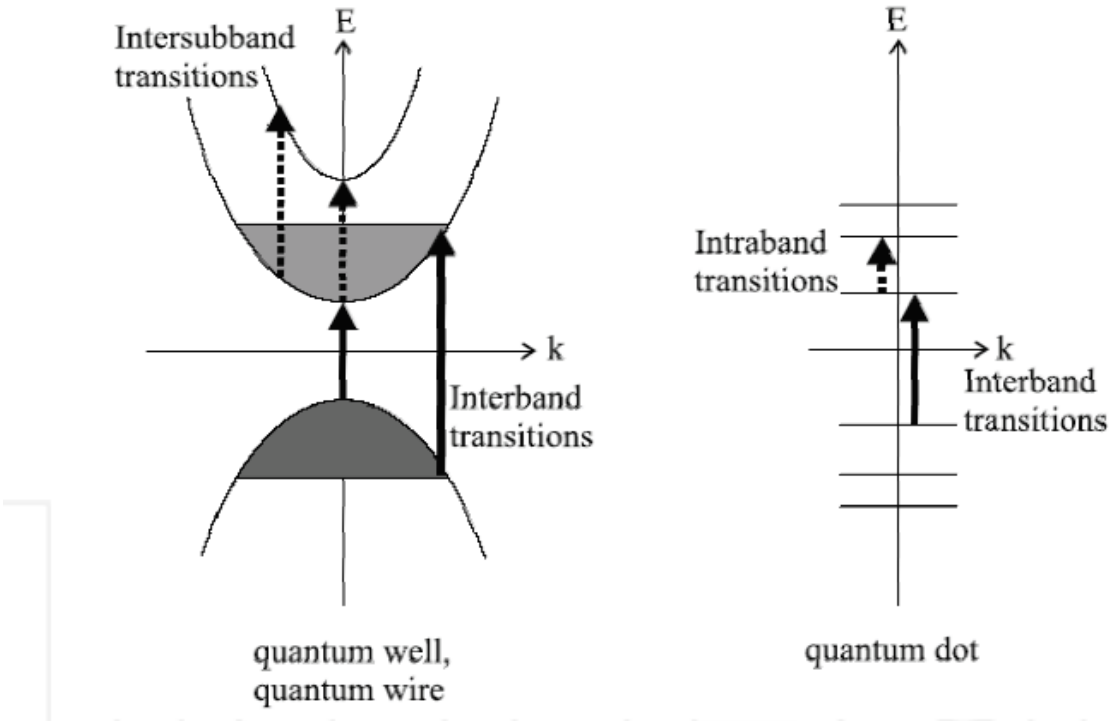

Fig.(2-2): (a) inter-sub-band transition in quantum well, wire. (b) in a quantum dot[72].

The discrete energy levels depending on the well width and the quantum number (n) as in the equation [73]

$$E_n = \frac{n^2\pi^2\hbar^2}{2m^*W^2} \qquad \text{n =1,2,3,....} \qquad (2\text{-}11)$$

W is the quantum well width

2.5 The optical confinement

One of essential parameters in semiconductor lasers "optical confinement factor Γ" defined as ratio of the intensity of the light existing in the active layer to the total light intensity in the outside active layer "cladding layer" or it is function of the electromagnetic energy of the guided mode in the active region [23, 74, 75]. It was also defined the fraction of the energy of a particular waveguide mode confined to the active layer, the confinement factor describe the overlap of the optically guided wave with the quantum well (QW), according to the formula

$$\Gamma = \frac{\int_{-w/2}^{w/2} \varepsilon_0^2(z)dz}{\int_{-\infty}^{+\infty} \varepsilon_0^2(z)dz} \qquad (2\text{-}12)$$

Where $\varepsilon_o(z)$ is the electrical field intensity of the first transverse mode TE_o generation in active layer [64, 76].

The optical confinement factor depending on thickness of active layer (d) unit (nm) , as well as it was function of well width (*W*) unit (nm), number of well (N_w) and barrier width (B) unit (nm)[70,77]. Analytical approximation for calculating the (Γ) in a symmetrical waveguide for the TE_o mode in Single Quantum Well (SQW) is given by [24, 76, 78]

$$\Gamma^{SQW} = \frac{C^2}{C^2+2} \qquad (2\text{-}13)$$

Where C is the normalized thickness of active region given by:

$$C = 2\pi \left(\frac{W}{\lambda}\right)\sqrt{(\gamma_{rw}^2 - \gamma_{rc}^2)} \qquad (2\text{-}14)$$

Here, λ is the wavelength and $\gamma_{rw,}\gamma_{rc}$ are the refractive indexes of active and cladding layers respectively. Therefore

$$\Gamma^{SQW} = \frac{(2\pi\left(\frac{W}{\lambda}\right)\sqrt{\gamma_{rw}^2-\gamma_{rc}^2})^2}{(2\pi\left(\frac{W}{\lambda}\right)\sqrt{\gamma_{rw}^2-\gamma_{rc}^2})^2+2} \qquad (2\text{-}15a)$$

$$\Gamma^{SQW} = \frac{2\pi^2 W^2(\gamma_{rw}^2-\gamma_{rc}^2)}{2\pi^2 W^2(\gamma_{rw}^2-\gamma_{rc}^2)+\lambda^2} \qquad (2\text{-}15b)$$

Significantly higher differences of refractive index can be achieved with heterostructures. For calculate the optical confinement factor of MQW structure can be use the following equation [74]

$$\Gamma^{MQW} = \Gamma^{SQW}\frac{N_w W}{d} \qquad (2\text{-}16)$$

Where d is average thickness of active region. Equation (2-16) can be achieve with homogeneous cladding layers and center layers of average thickness (d) with average index refraction (γ'_r) [75, 76]

$$\gamma'_r = \frac{N_w\, W\, \gamma_{rw}+N_b\, B\, \gamma_{rb}}{d} \qquad (2\text{-}17)$$

Where

$$d = N_w W + N_b B \qquad (2\text{-}18)$$

$$N_w = 1, N_b = 0 \qquad \text{for SQW} \qquad (2\text{-}19a)$$

$$N_b = N_w - 1 \qquad \text{for MQW} \qquad (2\text{-}19b)$$

The optical confinement factor of MQW, using C' instead of C in equation (2-13), which is given by:

$$C' = 2\pi\left(\frac{d}{\lambda}\right)\sqrt{\gamma'^2_r - \gamma_c^2} \qquad (2\text{-}20)$$

2.6 Optical Gain in semiconductor laser

The laser diode consists of a cavity which is the region between two mirrors (M_1, M_2) and the distance between M_1, M_2 called cavity length L[5]

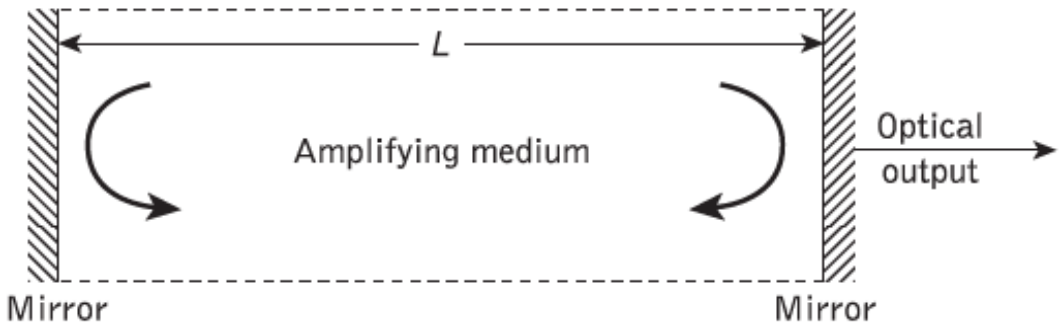

Fig.(2-3) the basic laser structure

$$L = m\frac{1}{2\gamma_{eff}}\lambda_0 \qquad \text{m=1,2,3,…..} \qquad (2\text{-}21)$$

γ_{eff} is the effective refractive index, λ_0 is the wavelength.

In the thermal equilibrium; the electrons exist in the valence band, holes exist in the conduction band and the Fermi level is in the middle band gap. The distribution of carriers in there bands is given by Fermi Dirac function:

$$f(E) = \frac{1}{exp[(E-E_f)/k_BT]+1} \qquad (2\text{-}22)$$

E, E_f, k_B are the energy level, the Fermi level energy and Boltzmann constant respectively, when laser diode is supplied with electrical current injection or pumping, the electron travels from the valence band to the conduction band behind created hole where many electrons exist in conduction band and many holes in valence band, Fig.(2-4).

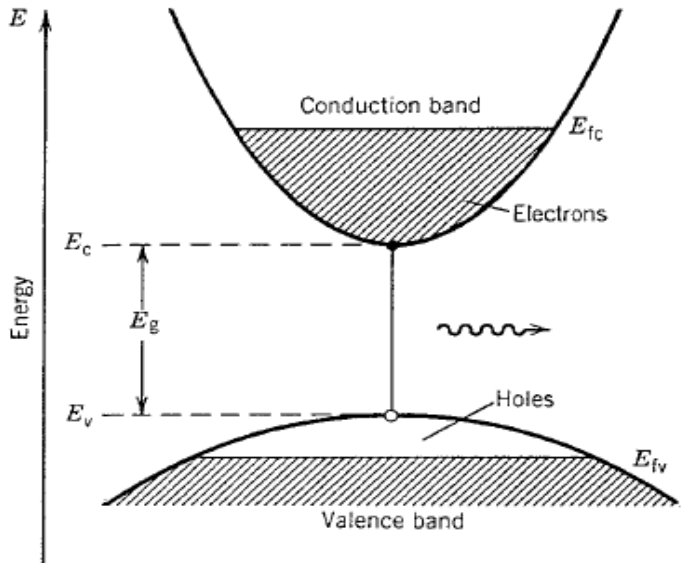

Fig.(2-4) the optical transition of electron in semiconductor [79]

The Fermi Dirac distribution function expressed for electron f_e and hole f_h as the following [64,79]

$$f_e = \frac{1}{\exp\left[\frac{(E_1 - E_{Fc})}{(k_B T)}\right] + 1} \qquad (2\text{-}23)$$

$$f_h = \frac{1}{\exp[(E_2 - E_{Fv})/(k_B T)] + 1} \qquad (2\text{-}24)$$

E_{Fv}, E_{Fc} are the quasi-Fermi level in conduction band and valence band are written as following:

$$E_{Fc} = E_c + k_B T ln(\frac{N_e}{N_c}) \qquad (2\text{-}25)$$

$$E_{Fv} = E_v + k_B T ln(\frac{P_h}{N_v}) \quad (2\text{-}26)$$

n, p are the concentration of electrons and holes respectively are given by[80].

$$N_e = N_c \exp(-\frac{E_c - E_{Fc}}{k_B T}) \quad (2\text{-}27)$$

$$P_h = N_v \exp(-\frac{E_v - E_{Fv}}{k_B T}) \quad (2\text{-}28)$$

N_c, N_v are the effective density of states for electrons in conduction band and holes in valence band respectively ,which are written as:

$$N_c = 2(\frac{2\pi m_e^* k_B T}{h^2})^{3/2} \quad (2\text{-}29)$$

$$N_v = 2(\frac{2\pi m_h^* k_B T}{h^2})^{3/2} \quad (2\text{-}30)$$

m_e^*, m_h^*, h are the effective mass of electron and hole, Plank's constant.

The fundamental of processes occurring between any two energy levels be (a) absorption (b) spontaneous emission (c) stimulated emission as in Fig(2-5) [79]

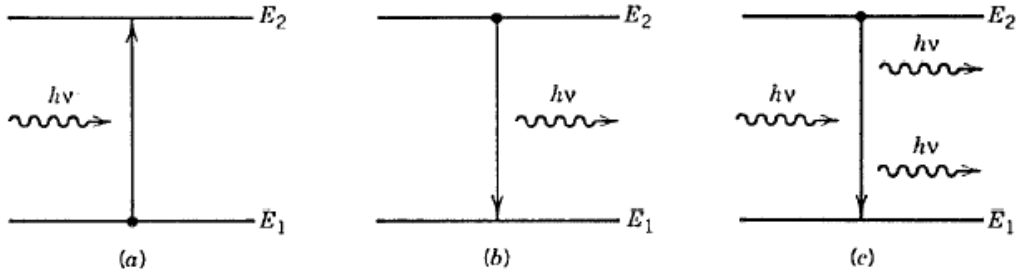

Fig.(2-5) (a) absorption (b) the spontaneous emission (c) the stimulated emission.

The optical gain occur when the stimulated emission rate more than the emission spontaneous rate and absorption rate.

$$R_{abs.} = B(E_{12}) \int [1 - f_c(E_2)] f_v(E_1) \rho_{cv} \rho_{ph} dE_2 \quad (2\text{-}31)$$

$$R_{spon.} = A(E_{21}) \int [1 - f_v(E_1)] f_c(E_2) \rho_{cv}\, dE \quad (2\text{-}32)$$

$$R_{stim.} = B(E_{21}) \int [1 - f_v(E_1)] f_c(E_2) \rho_{cv} \rho_{ph} dE \quad (2\text{-}33)$$

The net optical gain is written

$$R_{stim.} - R_{abs.} = B(E_{12}) \int (f_c - f_v) \rho_{cv} \rho_{ph} dE \quad (2\text{-}34)$$

where

ρ_{cv} are the joint density of states in conduction, valence bands

$$\rho cv = \frac{(2m_r)^{\frac{3}{2}}}{2\pi^2 \hbar^3} (\hbar\omega - E_g) \quad (2\text{-}35)$$

m_r is the reduce mass, ρ_{ph} is the density of photon respectively. The condition of laser, requirement the photon energy large than the band-gap $hv > E_g$ [44, 64, 79]

2.7 Threshold Condition for laser

There are three essential conditions that must realization in order to the laser devices operated, as shown in fig. (2-6) they are:

1-active medium "any material, solid, liquid or gas but in this work it is the semiconductor material

2-pumping process (or population inversion) "it is an energy input requirement to transition the electrons to higher level"

3-optical feedback "when the light produced in the laser medium is bounced back into the laser medium with help of two mirrors for amplification.

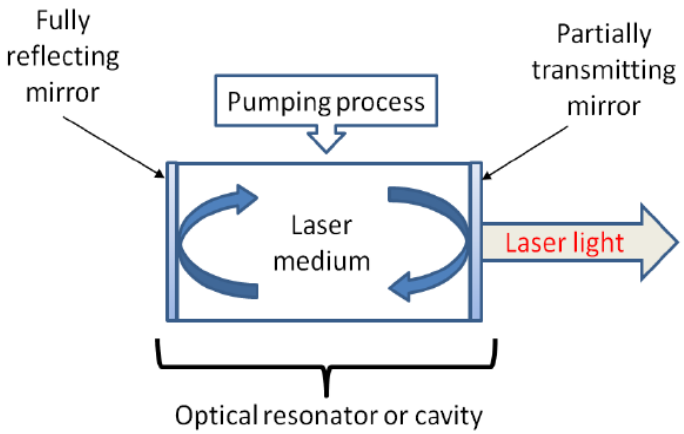

Fig. (2-6) the element of laser

The condition of laser in semiconductor action when the gain in the medium equal to total losses of laser structure, lasing will happen [44].The fractional loss written as [5]:

$$\text{Fraction loss}=R_1R_2\exp(-2\alpha L) \qquad (2\text{-}35)$$

R_1, R_2 are the refractivity of two mirror, α is the losses coefficient per unit length (cm^{-1}), L is the cavity length.

If the gain coefficient per unit length produced by stimulated emission the fractional round trip gain had been given by[44, 81] :

$$\text{Fractional gain}=\exp(2gL) \qquad (2\text{-}37)$$

$$\exp(2gL)\,R_1R_2\exp(-2\alpha L)=1 \qquad (2\text{-}38)$$

$$R_1R_2\exp[2(g-\alpha)L]=1 \qquad (2\text{-}39)$$

The optical gain at threshold, g_{th}, is equal to loss at threshold given by [81,82]:

$$G_{th}=\alpha_i+\frac{1}{L}ln\frac{1}{R} \qquad (2\text{-}40)$$

The local gain at threshold can be obtained from the following relation

$$g_{th} = \frac{1}{\Gamma_{MQW}}(\alpha_i + \frac{1}{L} ln \frac{1}{R}) \quad (2\text{-}41)$$

2.8 Threshold current

The first parameter is very important in laser diode device is the threshold current (I_{th}) depend upon the geometry of the device such as (area, size). When applied forward current, the device emitting some light output. This light operates with the properties of laser. In the small values of the applied current the emission will be corresponds for spontaneous emission and then will be threshold current after that will be emission corresponds for stimulated emission as in fig. (2-7)[81].

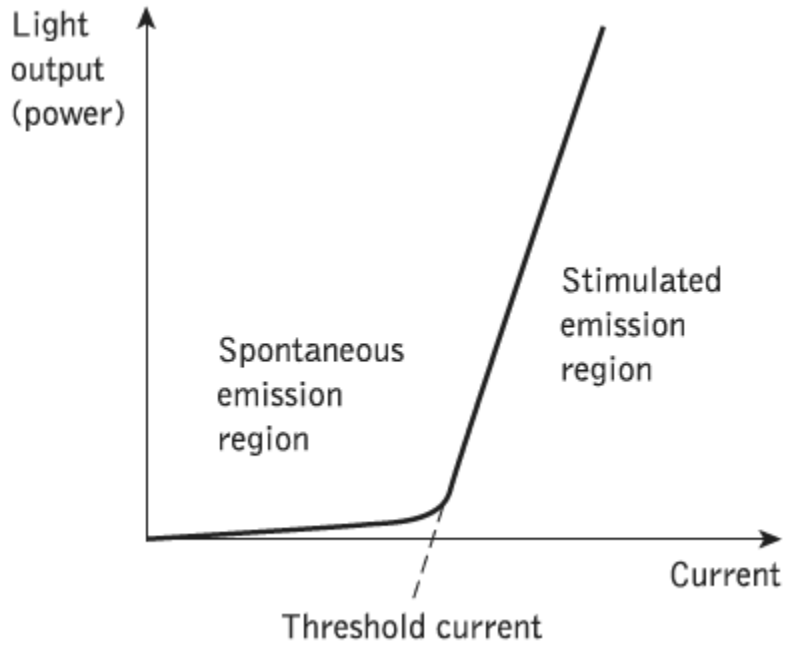

Fig.(2-7)light intensity against laser bias current, Showing threshold current[44]

When carriers are accumulated to from an inverted population the active layer exhibits optical gain and can amplify wave passing through it, the electromagnetic wave produce a full round trip in the cavity without attenuation, where the optical gain is equal for total losses which

free carrier absorption loss, scattering loss are called internal loss $\alpha_{int.}$ and mirror loss.

The small volume of active layer and higher gain in quantum confined lasers (QCs) can significantly decreasing their threshold currents[83]

In semiconductor laser, the gain coefficient at threshold g_{th} is calculated by the following equation [23].

$$\Gamma g_{th} = \alpha_{int} + \frac{1}{L} ln \frac{1}{R} \qquad (2\text{-}42)$$

In laser diode the optical gain has linear dependence upon bias current the following equation described the related between gain and current [10]

$$g = \frac{g_0}{J_0} \left(\frac{J\eta_{int.}}{d} - J_0 \right) \qquad (2\text{-}43)$$

Where (g_0, J_0) are constants and $\eta_{int.}$ the internal efficiency, through the above two equation we can obtain new parameter is the threshold current density J_{th}

$$J_{th} = \frac{J_0 d}{\eta_{int.}} \left\{ 1 + \frac{1}{g_0 \Gamma} \left[\alpha + \frac{1}{2L} \ln \left(\frac{1}{R_1 R_2} \right) \right] \right\} \qquad (2\text{-}44)$$

2.9 Threshold Current Density

The threshold current density of characteristic parameters in the operation laser diode it symbol J_{th} is determined by dividing the threshold current value I_{th} by the area A of the laser [84]

$$J_{th} = \frac{I_{th}}{A} \qquad (2\text{-}45)$$

There are many of the effectual parameters on the threshold current density, such as influence temperature, in application of a semiconductor laser the device is operate normally even at high temperature for measure the semiconductor laser sensitivity to (T) can use the characteristic temperature (T_0) threshold current density increase less rapidly with increasing (T) which the relationship between threshold current density and temperature is exponential function [44, 78].

$$J_{th} = J_0 \exp(\frac{T}{T_o}) \qquad (2\text{-}46)$$

J_0, T_0 are the saturation current density and characteristic temperature respectively .

And the second parameter is the optical confinement factor, $J_{th}$is the function of confined factor for single quantum well laser as shown the equation (2-44) [75]. In this equation observable the threshold current density decrease with increase $(\eta_{int.}, \Gamma \; and \; R)$ which (inverse relation) but threshold current density increase with increase active layer thickness d [10].

The reflectivity (R) for light of normal incidence reflected by mirror is given by

$$R = \left[\frac{\gamma_{re.2} - \gamma_{re.1}}{\gamma_{re.2} + \gamma_{re.1}}\right]^2 \qquad (2\text{-}47)$$

$\gamma_{re1}, \gamma_{re2}$ are the refractive index for dissimilar materials[44]. Last parameter is the output power increase with increase injection current and threshold current density, both p, J_{th} are proportional inverse with length cavity [74]. Also exist other away for calculate the threshold current density using the carrier concentration (N)

$$N_e = \frac{J}{qd}\tau_{Ne} \qquad (2\text{-}48)$$

τ_{Ne} is the carrier lifetime

When (N_e)arrived to threshold the threshold current density become the equation with new form

$$J_{th} = \frac{qd}{\tau_n}N_{th} \qquad (2\text{-}49)$$

Threshold current density is small when lifetime is long and threshold carrier concentration is small. We can re-write the equation as the flowing:

$$J_{th} = qdN_w B_{eff} N_{th}^2 \qquad (2\text{-}50)$$

Where

$$\frac{1}{\tau_{Ne}} = B_{eff}N_{th} \qquad (2\text{-}51)$$

B_{eff}, N_w are the effective recombination coefficient and threshold carrier density [10]

2.10 The Efficiency

There are several of important laser diode parameters, one of it is the parameter efficiency is determined performance of laser diode device, firstly we will explanation the internal quantum efficiency $(\eta_{int.})$ in converting electron-hole pairs (injection current) into photon (light) [81], or other expression is defined the number of photons emitted in laser cavity (inside) per injected carrier.

$$\eta_{int.} = \frac{N_{ph.}}{N_{inj.}} \qquad (2\text{-}52)$$

Where, N_{ph} is the number of photons emitted,$N_{inj}$is the number of injected electron[64,85]. Internal quantum efficiency is independent of the geometrical properties of the laser device example cavity length) but it depended on the device structure and material quality [10,84]. In active layer the internal efficiency is the fraction of electron-hole pairs that recombine radiatively [79].

$$\eta_{in} = \frac{\text{radiative recombination rate}}{\text{total recombination rate}} = \frac{R_r}{R_r+R_{nr}} = \frac{\tau_{nr}}{\tau_r+\tau_{nr}} \qquad (2\text{-}53)$$

τ_r, τ_{nr} are the radiative and nonradiative lifetime

The external efficiency (η_{ext}) is the ratio of the number of photon emitted outward ($N_{out\ ph.}$) to injected carrier ($N_{inj.}$)

$$\eta_{ext} = \frac{N_{out\,ph.}}{N_{inj.}} \qquad (2\text{-}54)$$

The parameter which measure the efficiency of getting the light out externally is the optical efficiency $\eta_{opt.}$ sometimes called external quantum efficiency $\eta_{ext.}$

$$\eta_{ext.} = \eta_{int.}\eta_{opt.} \qquad (2\text{-}55)$$

Or

$$\eta_{ext.} = \eta_{int.}\eta_{extraction} \qquad (2\text{-}56)$$

The extraction efficiency $\eta_{extraction}$ is the ratio of the production photon in quantum well that can be extracted out from device to the free space [85]. External quantum efficiency can be written in another way:

$$\eta_{ext.} = \eta_{int.}\frac{\alpha_m}{\alpha_i+\alpha_m} = \eta_{int.}\frac{\frac{1}{L}ln\frac{1}{R}}{\alpha_i+\frac{1}{L}ln\frac{1}{R}} \qquad (2\text{-}57)$$

External quantum efficiency is always smaller than the internal efficiency[81,84-86], the external efficiency can be written as follows[34, 87]

$$\eta_{ext.} = \frac{q}{\hbar\omega}\frac{\Delta P}{\Delta I} \qquad (2\text{-}58)$$

Where ω is the angular frequency $\Delta P, \Delta I$ are the increase in light intensity and injected current respectively ,which exist relation between the external efficiency and slope efficiency η_{slope} is the increase in light intensity per increase in injected current with unit (W /A)

$$\eta_{slope} = \frac{\Delta P}{\Delta I} \qquad (2\text{-}59)$$

2.11 Output Power

The basic laser characteristic is the measurement of the light output power. Also from lasing condition is the threshold current (I_{th}), the light emitted of down threshold current is very small. The power generated by stimulated emission internally is linearly dependent upon the applied current as in Fig(2-8), [10,88]

$$P_{stim.} = \eta_{int.}\frac{h\upsilon}{q}(I - I_{th}) \qquad (2\text{-}60)$$

$h\upsilon$ is photon the energy , $\eta_{int.}$ is the internal efficiency

$$P_{out} = P_{stim.}\frac{(\frac{1}{2L})\ln(\frac{1}{R_1R_2})}{\alpha+(\frac{1}{2L})\ln(\frac{1}{R_1R_2})} \qquad (2\text{-}61)$$

P_{out} is the output power

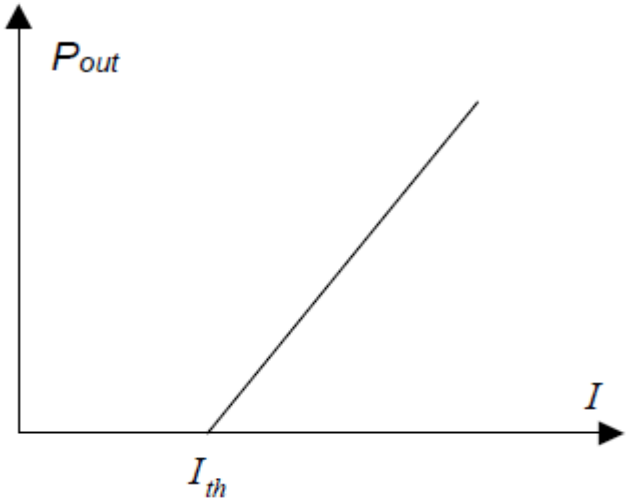

Fig.(2-8) Output power for laser diode with applied current

As well as we can describe the behavior of semiconductor laser by the rate equation (for both photon and electron density (φ)) that control interaction of photon and electron in the active region of the structure [5].

$$\varphi = \frac{\tau_{ph}}{qd}(J - J_{th}) \qquad (2\text{-}62)$$

$$\eta_{ext.} = \eta_{slop}\left(1 - \frac{I_{th}}{I}\right) \qquad (2\text{-}63)$$

Where

$$\eta_{slop} = \frac{\Delta P}{\Delta I}$$

$$P_{out} = \eta_{int.} E_g \left[\frac{ln\frac{1}{R_1R_2}}{2\alpha L + ln\frac{1}{R_1R_2}}\right](I - I_{th}) \qquad (2\text{-}64)$$

But the optical power per unit area is given by:

$$P_{out} = \eta_{int.} E_g \left[\frac{ln\frac{1}{R_1R_2}}{2\alpha L + ln\frac{1}{R_1R_2}}\right](J - J_{th}) \qquad (2\text{-}65)$$

CHAPTER THREE

RESULTS AND DISCUSSION

3.1 Introduction

This chapter includes the Results which are obtained through applying the expression, which are shown in chapter two. Where the Calculation and simulate for structure parameters such as well width, barrier width and the laser diode parameters such as density of states, the optical confinement factor, the optical gain, threshold current density and output power. All these parameters are calculated for Multi Quantum Well of $Al_{0.3}Ga_{0.7}As$/GaAs and $Hg_{0.2}Cd_{0.8}Te/Hg_{0.5}Cd_{0.5}Te$ heterostructures laser systems and these two systems can be compared

3.2 Scope of the Work

The materials used in this work are $Al_{0.3}Ga_{0.7}As$/GaAs and $Hg_{0.2}Cd_{0.8}Te/Hg_{0.5}Cd_{0.5}Te$ as a multi quantum heterostructure laser systems. We chose *GaAs* as a standard material because the studies proved that *GaAs* is the best material for produce the laser, the semiconductor material HgCdTe was chosen to comparison with GaAs, because it is widely used for high performance IR photodetectors [43]. The $Hg_{0.5}Cd_{0.5}Te$ using in this work due to it has constant energy gap for difference temperature. Also it is emitting long wavelength which use in many applications as (communication system and detection devices).

We know the MQW consist of wells and barriers. The material of well layer in the first system is GaAs, barrier layer is $Al_{0.3}Ga_{0.7}$As and $AlAs$ is the cladding layers. The material of well layer in the second system is $Hg_{0.5}Cd_{0.5}Te$ while the barrier layer is $Hg_{0.2}Cd_{0.8}Te$ and the cladding layer is $Hg_{0.1}Cd_{0.9}Te$. Matlap version 8.1 (2013) was used to draw the figures and calculation. Scope of this work is illustrated as the block diagram,the laser parameters and constants which will be used in the calculation needed in this chapter are listed in table (3-1) (3-2) and (3-3)

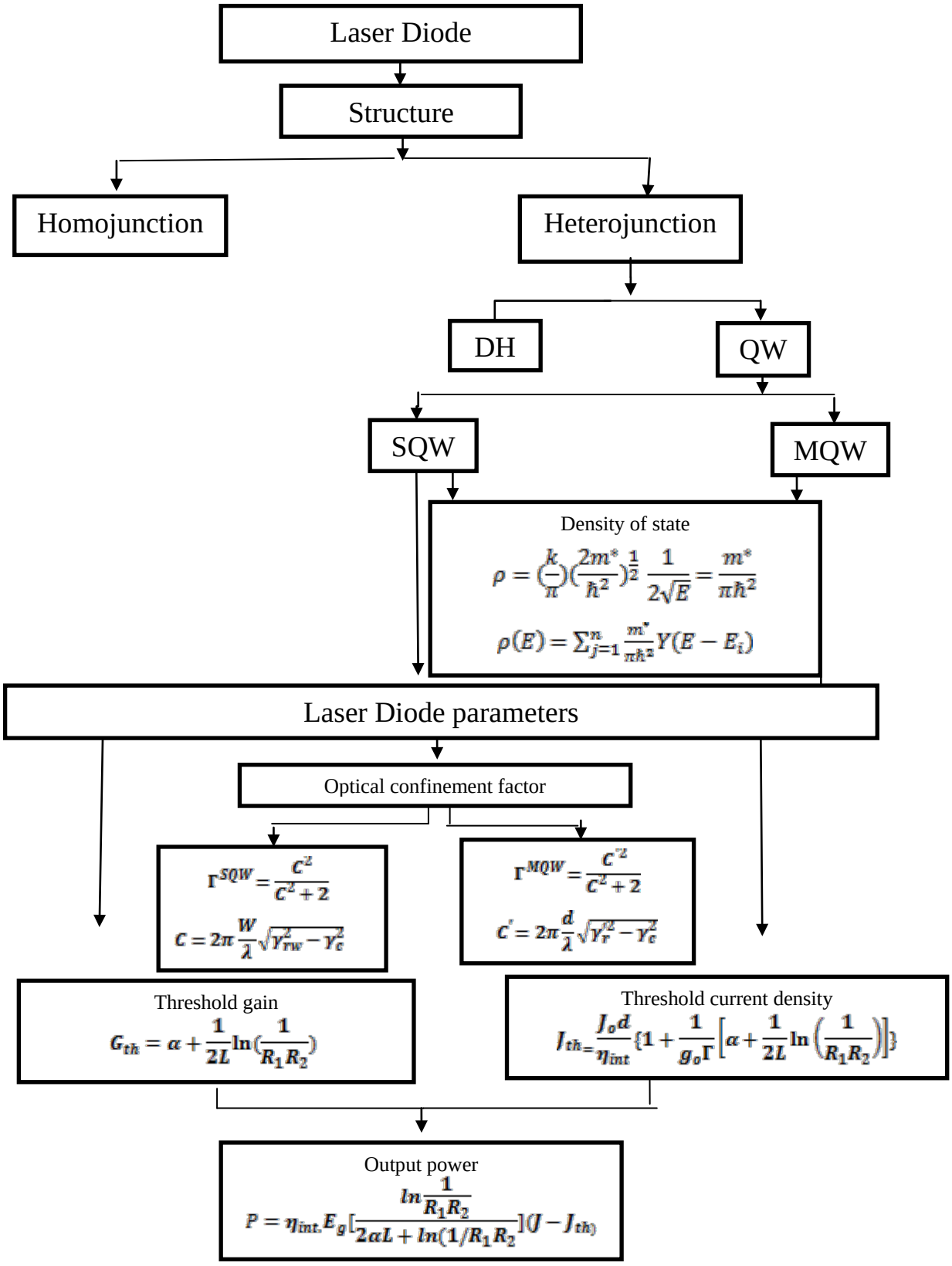

Fig.(3.1) Block diagram which is summarizing our work on the theoretical investigation of the parameters affecting for laser diode.

Table (3-1) list of constant

Constant	Values	Unit
q	1.6×10^{-19}	C
h	6.626×10^{-34}	J.s
K_B	1.38×10^{-23}	J/K
T	300	K
L	2	μm

Table (3-2) properties of GaAs

Constant	Values	Unit	Ref.no
λ	872	nm	[23]
E_g	1.424	eV	Eq.(1-1)
m_e^*	5.733×10^{-32}	kgm	[10]
γ_r	3.59	none	Eq.(1-2)
J_o	4.51×0^3	$A/cm^2.\mu m$	[10]
g_o	225	cm^{-1}	[10]
N_w	3	none	
α_i	10	cm^{-1}	[89]

Table (3-3) properties of $Hg_{0.5}Cd_{0.5}Te$

Constant	Value	Unit	Ref.No
λ	2200	nm	[23]
E_g	0.5645	eV	eq.(1-3)
m_e^*	3.9565×10^{-32}	kgm	[32]
γ_r	3.1322	none	Eq. (1-5)
J_0	1.5564×10^4	$A/cm^2.\mu m$	Evaluation from[53]
g_0	1.3883×10^5	cm^{-1}	Evaluation from[50]
N_w	5	none	
α_i	15	cm^{-1}	Evaluation from [90]

3.3 Density of state

The density of state as a function of energy for bulk and semiconductor quantum well is shown in the fig. (3-2) using the equations (1-6) and (1-8). Note that the dashed curve for bulk semiconductor, which density of state increasing with increasing of the energy (continue), while the density of states for a quantum well is a step function with steps occurring at the energy of each quantized level

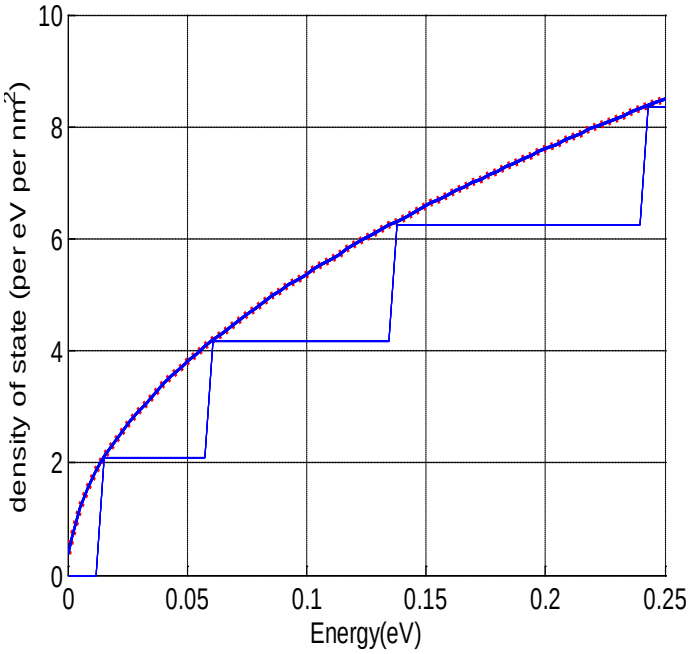

Fig. (3-2) the density of the state as a function of the energy

3.4 Parameters Affecting the Optical Confinement Factor

3.4.1 The Well Width (*W*)

The optical confinement factor for $Al_{0.3}Ga_{0.7}As/GaAs$ and $Hg_{0.2}Cd_{0.8}Te/Hg_{0.5}Cd_{0.5}Te$ Multi-quantum well systems was calculated from implementation equations (2-13) and (2-16).

The variation of this factor with well width for these two systems is illustrated in Fig. (3-3) and (3-4) for several barrier widths (2, 5, 10, 15,

20) nm. In each figure there are three cases of well number (3, 4, 5). It's clear from these figures that the optical confinement factor (Γ)is increasing with increases well width for all values of the barrier width. Also for all values of barrier width there is the same value of Γ for particular value of well width for each case. However, for well width less than this particular value, it become clear that the changing rate of optical confinement factor with increasing barrier width can be neglected, while above this value the changing rate of Γ for barrier width of 2 nm is more than of other barriers.

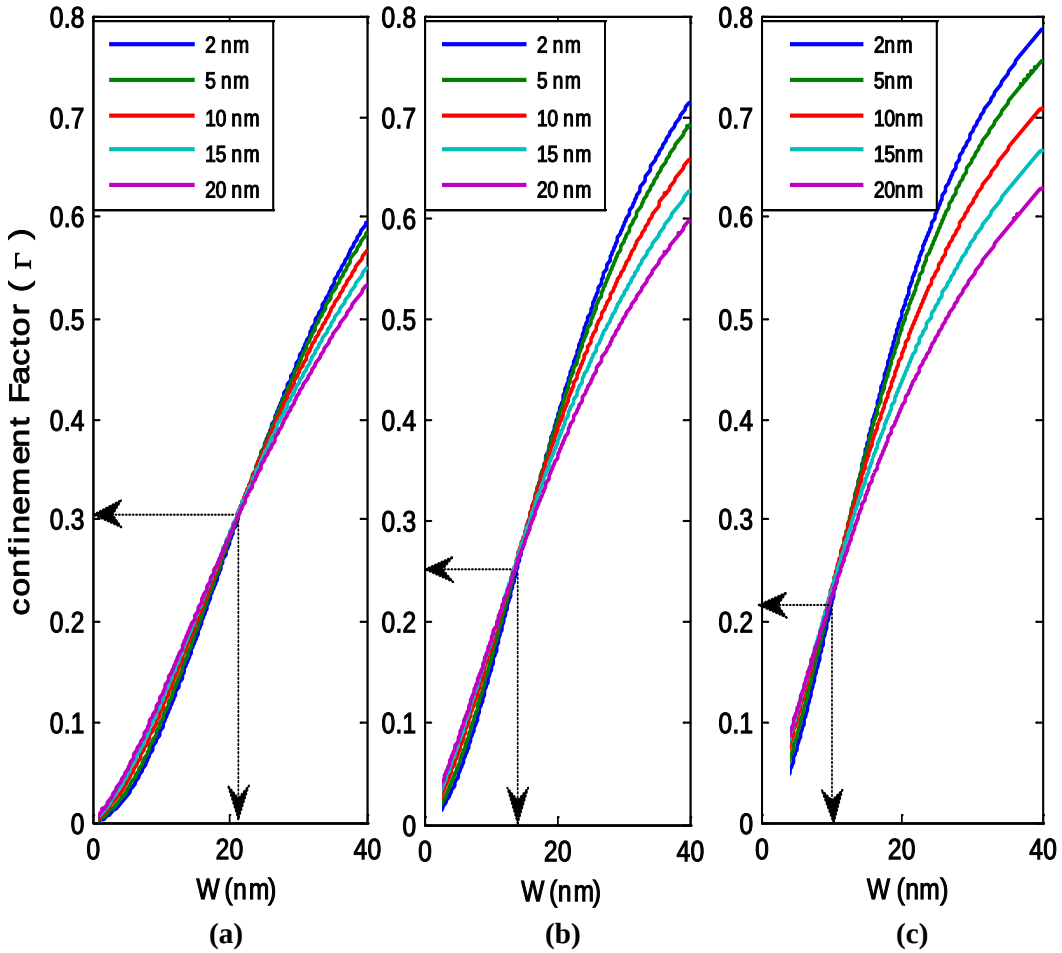

Fig. (3-3) the optical confinement factor as function of well width for different barrier width for MQW $Al_{0.3}Ga_{0.7}As/GaAs$(a:$N_w = 3$, b: $N_w = 4$and c: $N_w = 5$)

We show in fig. (3-3), case (a) well number is three, the well width is (W=21.5nm) and optical confinement factor is $\Gamma = 0.308$ while in the

case (b) well number is four, the well width is (*W*= 14.5nm) and the optical confinement factor is $\Gamma = 0.268$ at last case (c) number of well is five where the well width is (*W*=10nm) and $\Gamma = 0.224$. We note from these cases that the optical confinement factor has larger value at well number ($N_w = 3$). The fig.(3-3) for $Hg_{0.2}Cd_{0.8}Te/Hg_{0.5}Cd_{0.5}Te$ multi quantum well structure.

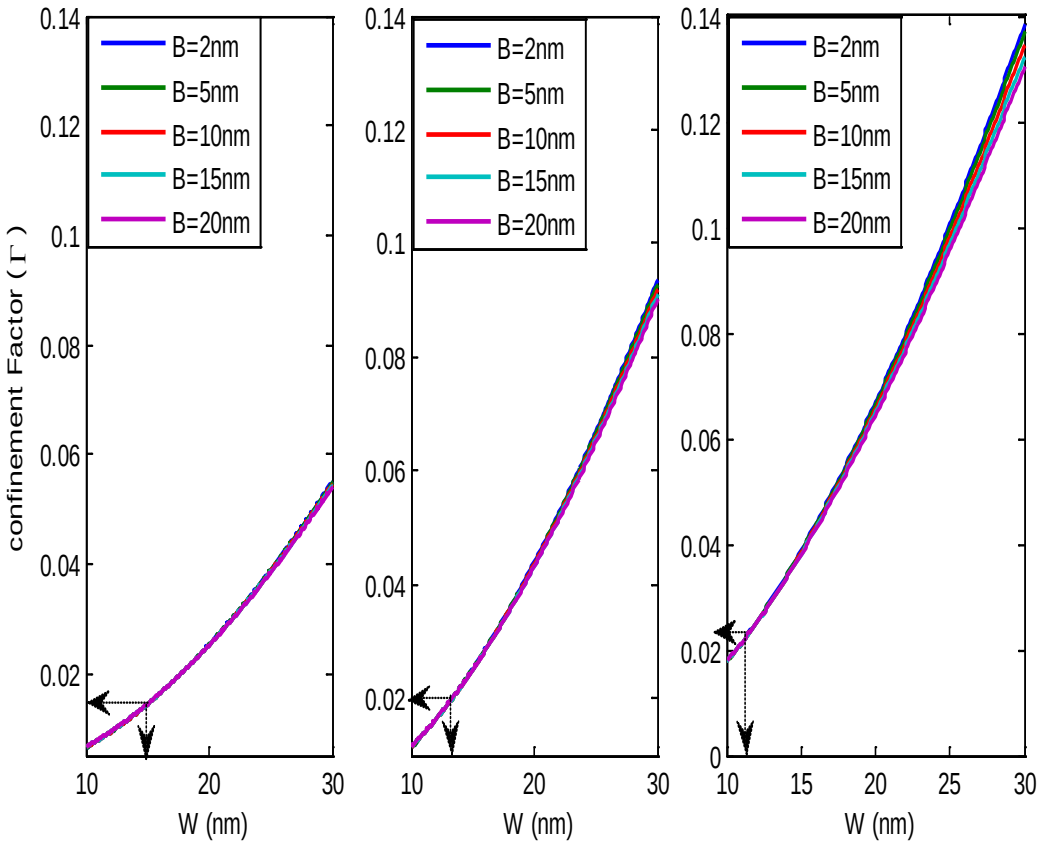

Fig (3-4) the confinement factor as function of well width for different barrier width for the $Hg_{0.2}Cd_{0.8}Te/Hg_{0.5}Cd_{0.5}Te$ MQW(a:$N_w = 3$, b: $N_w = 4$and c: $N_w = 5$)

It's clear from this figure that the optical confinement factor for (N_w =3) and well width (15nm) is 0.0144 while for (N_w =4) with well width (13.2nm) is 0.0196 and at $(N_w = 5)$, well width (11.3nm), the optical confinement factor is 0.0224. It's apparent that the optical confinement factor is larger at $(N_w = 5)$Thus we used material GaAs

with number of well (3), and $Hg_{0.5}Cd_{0.5}Te$ with number of well (5) are studying in order to compare.

3.4.2 The Barrier width

The effect of the barrier width (B) on the optical confinement factor was calculated by using eq. (2-16), (2-17) and (2-18). The dependence of this factor on barrier width for different well with [5,10,15,20,21.5, 25,30]nm for $Al_{0.3}Ga_{0.7}As/GaAs$ 3QWs is illustrated in fig.(3-5).

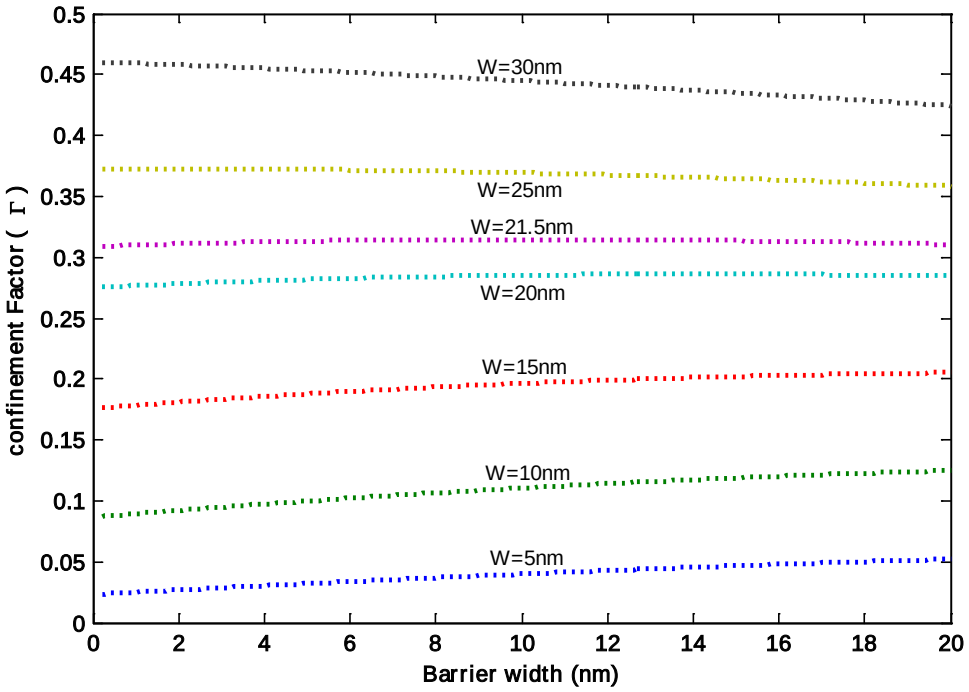

Fig.(3-5) the optical confinement factor as a function of barrier width for $Al_{0.3}Ga_{0.7}As/GaAs$ 3QWs

We note best value for well width (W=21.5nm) and around (Γ =0.307). When the well width less than 21.5nm the optical confinement factor is increasing with increases barrier width, but for well width (W=21.5nm) the optical confinement factor is approximately constant around the value 0.308, while well width (W=25 and30 nm) the optical

confinement factor decreases with increasing of barrier width for the same range of the barrier widths.

Fig.(3-6) for $Hg_{0.2}Cd_{0.8}Te/Hg_{0.5}Cd_{0.5}Te$ MQW system, With well width [5,10,11.3,12, 15and 20 nm] the optical confinement factor is increasing slightly for well width less than 11.3 nm, but for well width 11.3 nm the optical confinement factor is approximate constant at 0.0224 for the same barrier width range. While, for well width more than 11.3 nm the optical confinement factor decreases with increasing of the barrier width.

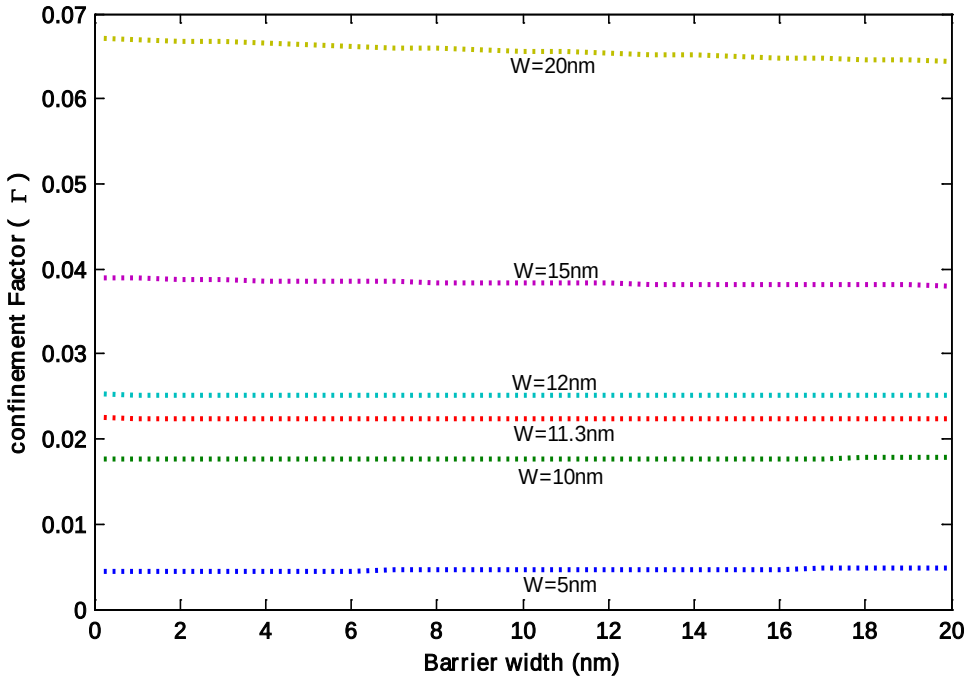

Fig. (3-6) the optical confinement factor as a function of barrier width for $Hg_{0.2}Cd_{0.8}Te/Hg_{0.5}Cd_{0.5}Te$ 5QWs

Therefore we choose well width 21.5nm with barrier width 2nm for $Al_{0.3}Ga_{0.7}As/GaAs$ 3QWs and well width 11.3nm with B=2nm for $Hg_{0.2}Cd_{0.8}Te/Hg_{0.5}Cd_{0.5}Te$, 5QWs systems as typical values for our two structures.

3.4.3 Single and Multi Quantum well

Fig. (3-7) illustrates the difference between the values of Γ for Single quantum well (SQW) and multi quantum well (MQW) for two systems ($Al_{0.3}Ga_{0.7}As/GaAs$ and $Hg_{0.2}Cd_{0.8}Te/Hg_{0.5}Cd_{0.5}Te$) at each value of well widths calculated from eqs. (2-13) and (2-16). It's clear from this figure that the optical confinement factor for SQW is very small comparison with Γ for three quantum wells. Where Γ =0.017 for well width 21.5nm with barrier width 2nm comparison with Γ =0.307 for multi quantum well for the same well width and barrier width for $Al_{0.3}Ga_{0.7}As/GaAs$ as shown in fig.(3-7a). Also for $Hg_{0.2}Cd_{0.8}Te/Hg_{0.5}Cd_{0.5}Te$ Fig.(3-7b), We note or notice that the optical confinement factor for SQW for *W*=11.3nm and *B*=2nm is 8.8×10^{-4} while for the 5QWs structure is 0.0224 for the same value of *W* and *B*. Because the optical confinement factor for SQW structure is depending on W^2 while MQW is depending on d'^2. Optical confinement factor of 3QWs are higher by a factor 18 for $Al_{0.3}Ga_{0.7}As/GaAs$ and by a factor 25 for $Hg_{0.2}Cd_{0.8}Te/Hg_{0.5}Cd_{0.5}Te$ 5QWs than optical confinement factor of SQW. Therefore the optical confinement factor for SQW is neglected, due to Γ for SQW very smaller than Γ for MQW.

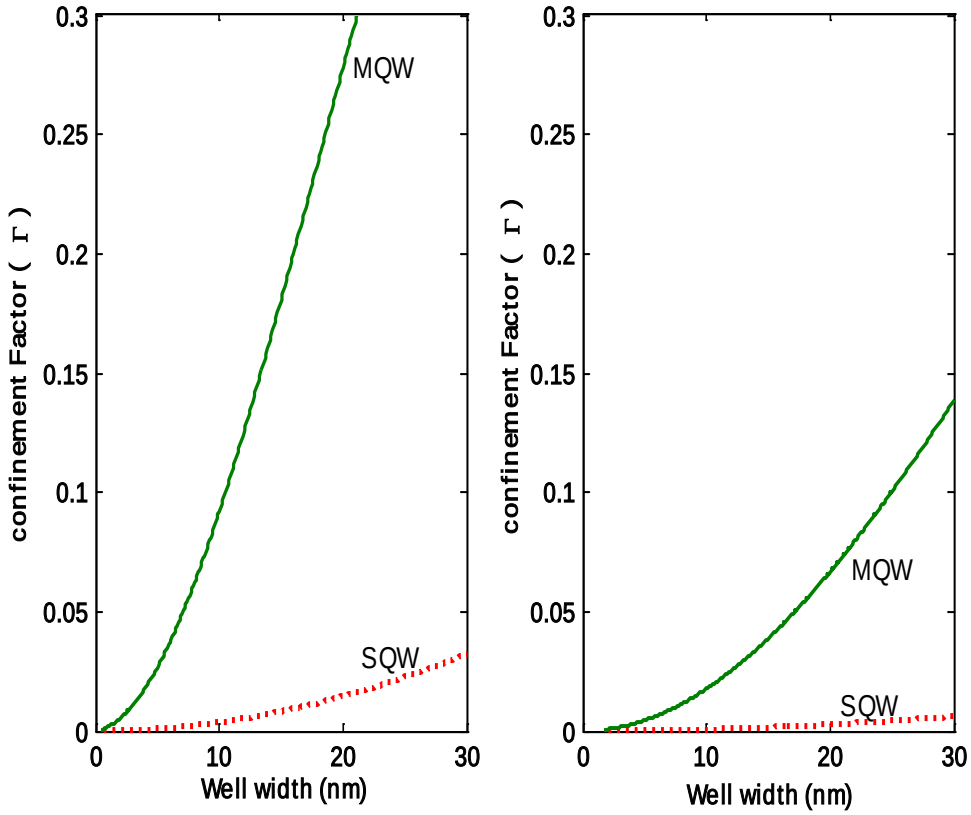

Fig. (3-7) the optical confinement factor as a function of well width for SQW and MQW for (a): $Al_{0.3}Ga_{0.7}As/GaAs$. (b): $Hg_{0.2}Cd_{0.8}Te/Hg_{0.5}Cd_{0.5}Te$ systems.

3.5 Intersubband Transition

The optical confinement factor for electron intersubband transition in conduction band was calculated for $Al_{0.3}Ga_{0.7}As/GaAs$ and $Hg_{0.2}Cd_{0.8}Te/Hg_{0.5}Cd_{0.5}Te$ MQW systems as a function of well width by using the eqs. (2-11), (2-16) and (2-20). The results are presented in Fig.(3-8) and Fig. (3-9) for allowed intersubband transition $(\Delta n = 1)$.

It is clear that the optical confinement factor values are high, but, at opposite the small values for well width this lead to emission short wavelengths with high energy this is disagree with our aim for obtain a longe wavelength, additionally, the risk of radiation with high energy must be avoid.

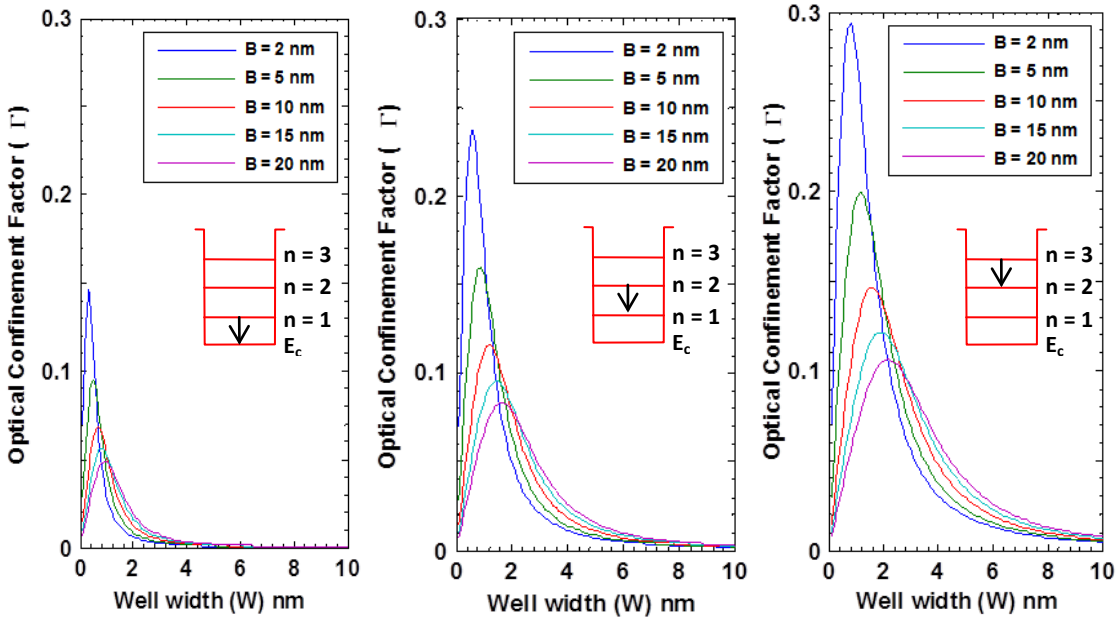

Fig. (3-8) intersubband transitions for $Al_{0.3}Ga_{0.7}As/GaAs$ 3QWs.

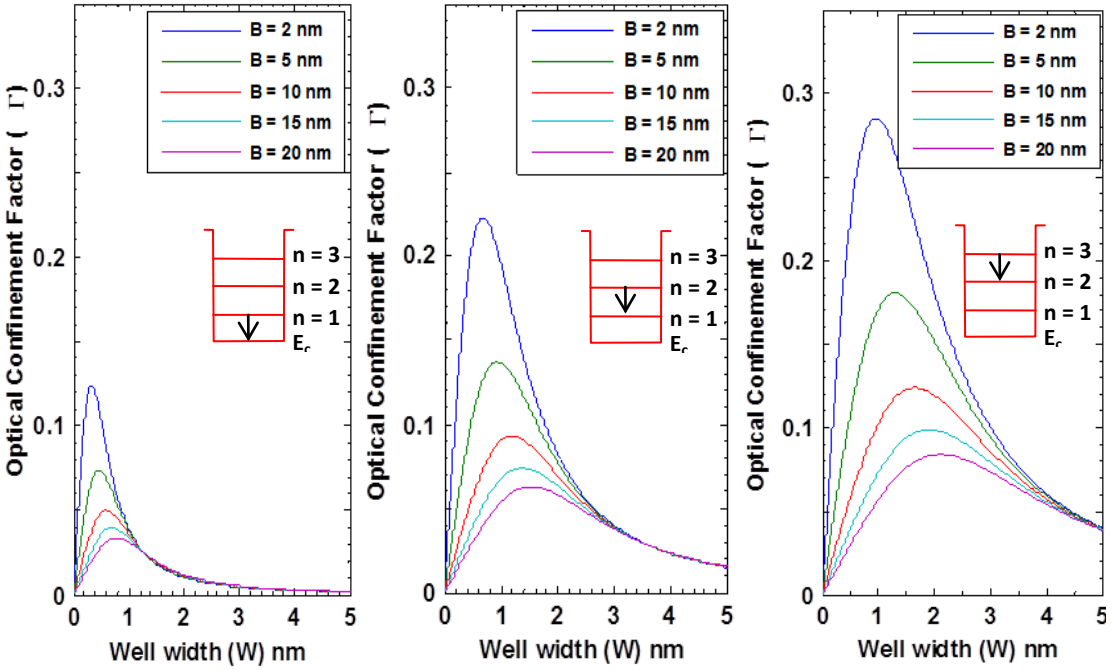

Fig. (3-9) intersubband transitions for $Hg_{0.2}Cd_{0.8}Te/Hg_{0.5}Cd_{0.5}Te$ 5QWs.

3.6 Parameters Affecting the Threshold current density

The threshold current density is the basic parameter of laser diode. There are several of parameters affecting the threshold current density such as:

3.6.1 Well width

The well width influence threshold current density, J_{th}, where J_{th} decreases with increasing well width until arriving the minimum value and then increases with increasing well width as shown in the Fig. (3-10). This figure plotted by calculated J_{th} from eq. (2- 44) for two different barrier width (2and 20nm) and the reflectivity are $R_1 = 0.9$ and $R_2 = 0.7$.

It is apparent that the best value of $J_{th} = 5784\, A/cm^2$, *W*=30nm for $Al_{0.3}Ga_{0.7}As/GaAs$ 3QWs and $J_{th} = 1327\, A/cm^2$ *W*=8 nm for $Hg_{0.2}Cd_{0.8}Te/Hg_{0.5}Cd_{0.5}Te$ 5QWs. But for SQW that the $J_{th} = 2.812 \times 10^4 A/cm^2$at well width (153nm) for$Al_{0.3}Ga_{0.7}As/GaAs$ and $J_{th} = 7805\, A/cm^2$ at well width (46nm) for$Hg_{0.2}Cd_{0.8}Te/Hg_{0.5}Cd_{0.5}Te$. We show that J_{th} for $Al_{0.3}Ga_{0.7}As/GaAs$ larger than J_{th} for $Hg_{0.2}Cd_{0.8}Te/Hg_{0.5}Cd_{0.5}Te$.

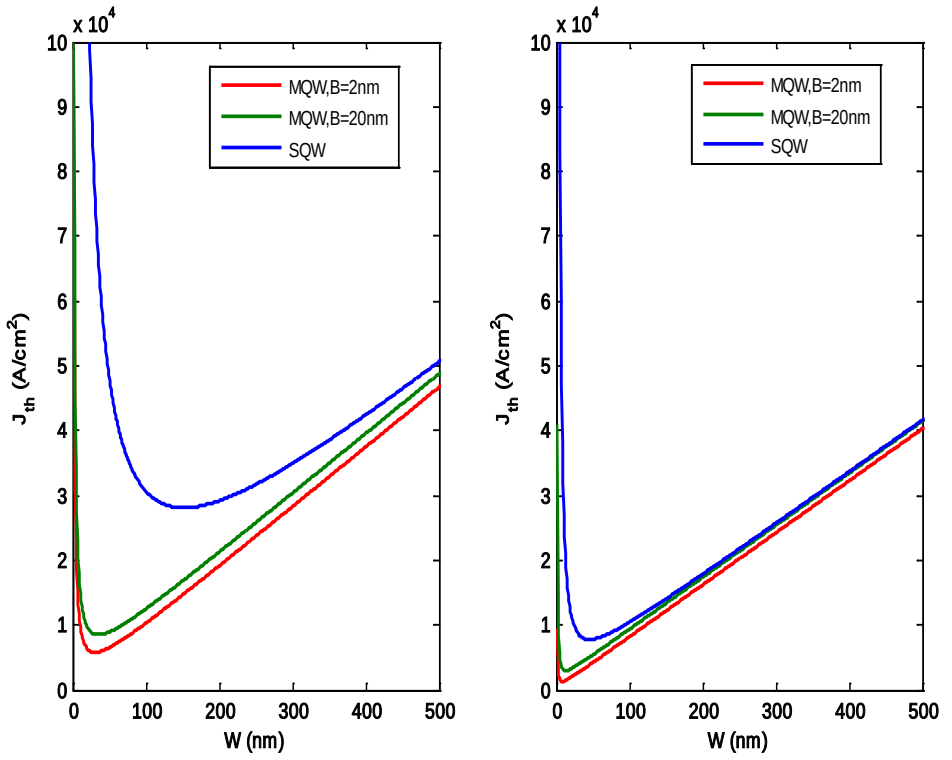

Fig. (3-10) Threshold current density as a function of well width for B (2, 20nm), where R_1=0.9 and R_2=0.7.

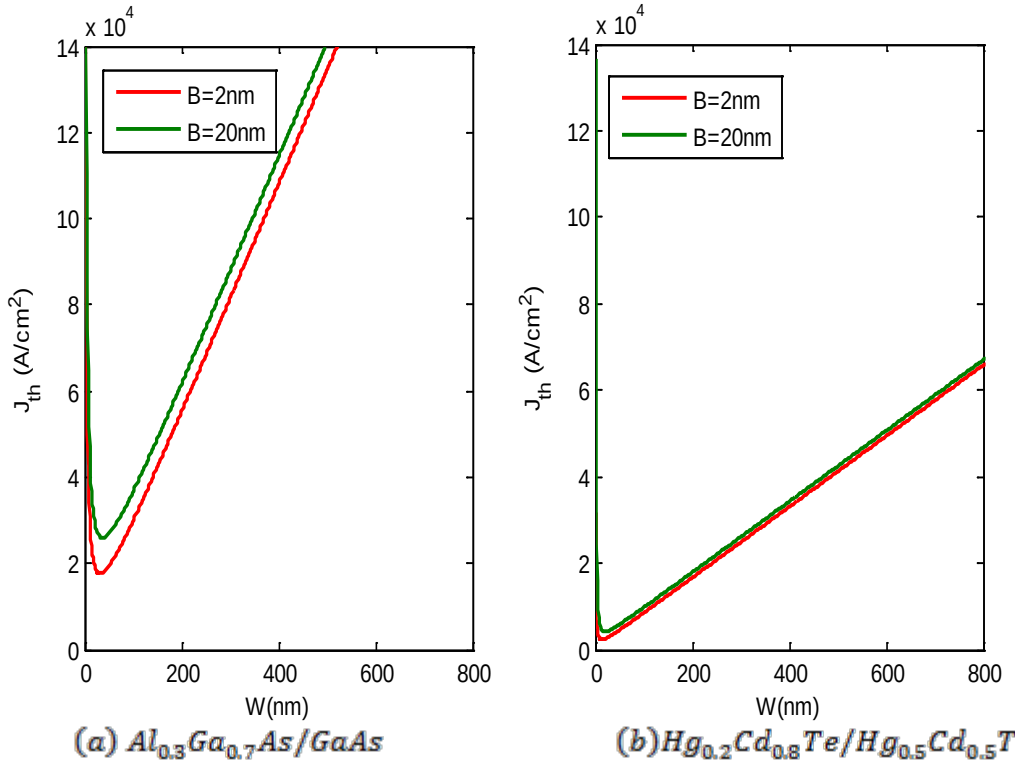

Fig. (3-11) Threshold current density as function of well width for B (2, 20nm), where R_1=0.9 and R_2 =eq. (2-47)

Fig.(3-11) shows a plot of J_{th} versus W for two different B (2and 20nm) too, but $R_1 = 0.9$ and $R_2 = eq.(2-47)$.We found that the values of threshold current density for $Al_{0.3}Ga_{0.7}As/GaAs$ is $1.769 \times 10^4 A/cm^2$ and for $Hg_{0.2}Cd_{0.8}Te/Hg_{0.5}Cd_{0.5}Te$ is $2290\ A/cm^2$.

3.6.2 The optical confinement factor

The threshold current density as a function of the optical confinement factor, for two different barrier widths (2, 20nm) was calculated by using eqs. (2-44) and (2-16). The variations of the results obtained are shown in fig. (3-12), in which the threshold current density is, drown with $R_1 = 0.9$ and $R_2 = 0.7$.

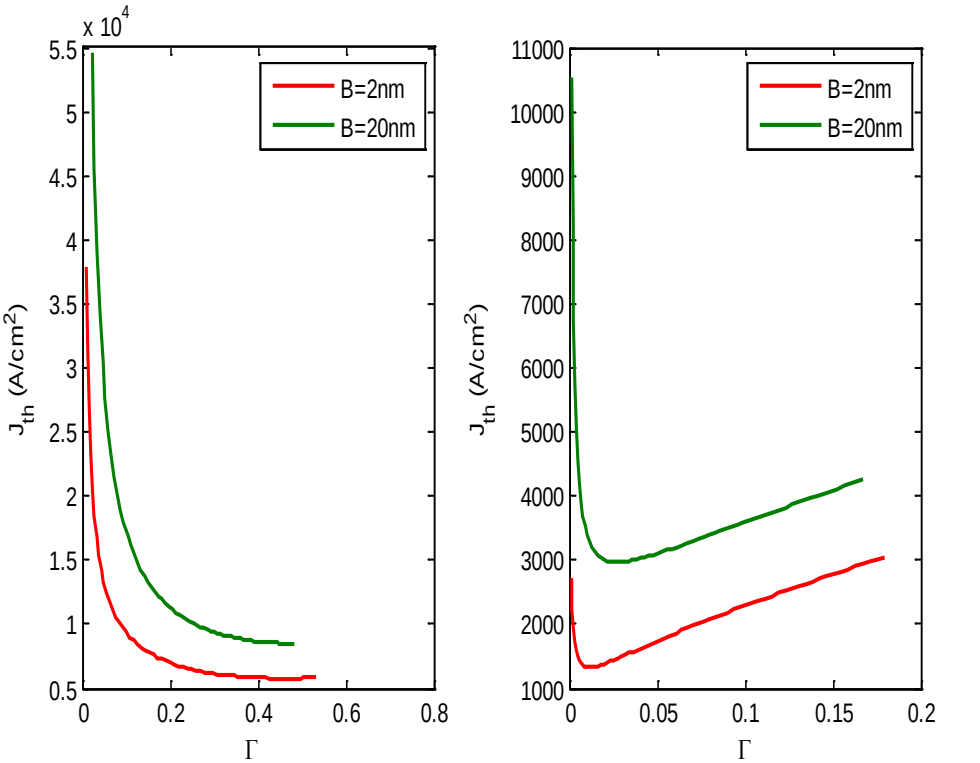

(a) $Al_{0.3}Ga_{0.7}As/GaAs$ (b) $Hg_{0.2}Cd_{0.8}Te/Hg_{0.5}Cd_{0.5}Te$

Fig. (3-12) threshold current density as function of optical confinement factor with two different barrier widths (2 and 20nm) for:(a) $Al_{0.3}Ga_{0.7}As/GaAs$. (b) $Hg_{0.2}Cd_{0.8}Te/Hg_{0.5}Cd_{0.5}Te$

It is clear that threshold current density for $Al_{0.3}Ga_{0.7}As/GaAs$ MQW is 5784 A/cm^2 with optical confinement factor 0.458 for barrier width 2nm which thinner barrier width, lower threshold current density is obtained, While in $Hg_{0.2}Cd_{0.8}Te/Hg_{0.5}Cd_{0.5}Te$ MQW the threshold current density is 1327$A/cm^2$for the optical confinement factor is 0.01137 and barrier width 2nm. We note that at small barrier width, the threshold current density is small too.

The fig.(3-13) explains threshold current density for $AlGaAs$ and $HgCdTe$ for two different barrier width but with variation reflectivity as $R_1 = 0.9$ and $R_2 = eq.(2-47)$.

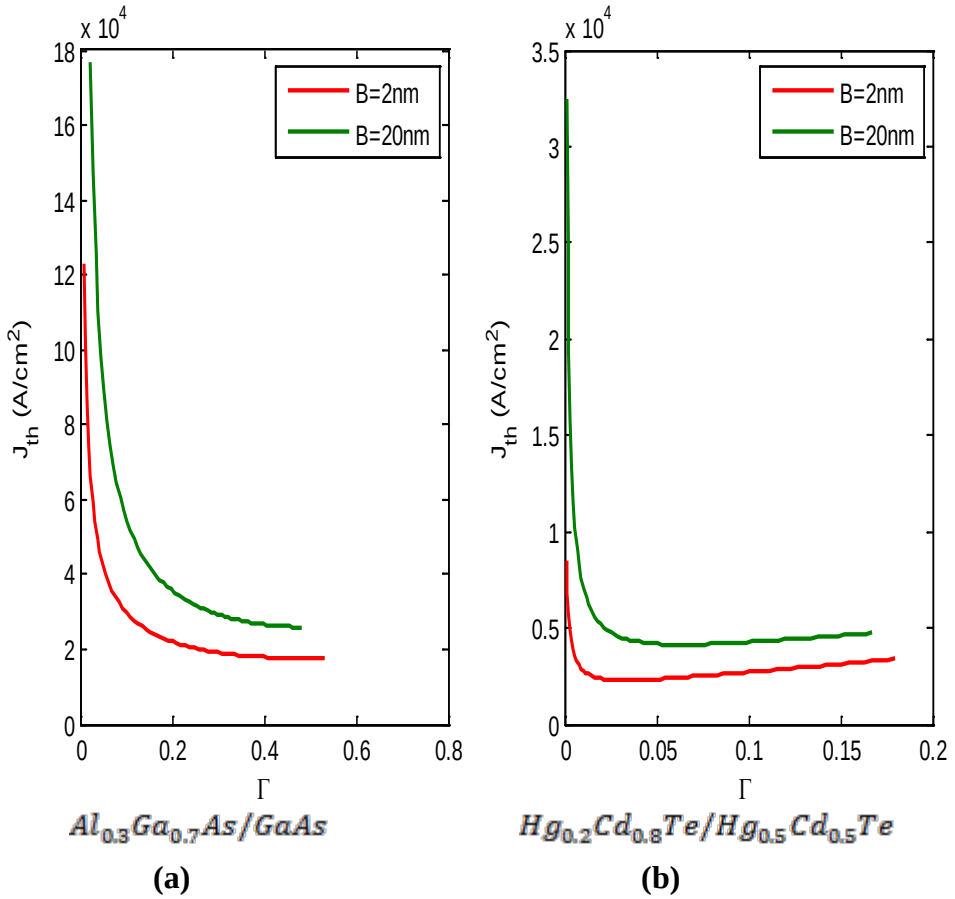

Fig. (3-13) threshold current density as a function of confinement factor with two different barrier widths for: (a) $Al_{0.3}Ga_{0.7}As/GaAs$ 3QWs and (b) $Hg_{0.2}Cd_{0.8}Te/Hg_{0.5}Cd_{0.5}Te$ 5QWs.

Where the $J_{th} = 1.797 \times 10^4\ A/cm^2$ at $\Gamma = 0.3992$ for the material AGaAs and $J_{th} = 2298 A/cm^2$ for the $\Gamma = 0.0585$ for the material $HgCdTe$, We can notice from these four last figures that J_{th} when we used $R_1 = 0.9$ and $R_2 = 0.7$ is smaller than J_{th} when we used $R_1 = 0.9$ and $R_2 = \text{eq.}\,(2-47)$ because the increase of reflectivity lead to increase the feedback of produce laser. Therefore we neglected $R_2 = (2-47)$ and used $R_2 = 0.7$.

3.6.3 Threshold Gain

Threshold current density as function of threshold gain for $Al_{0.3}Ga_{0.7}As/GaAs$ and $Hg_{0.2}Cd_{0.8}Te/Hg_{0.5}Cd_{0.5}Te$ MQW structures as shown in figure (3-14) we note that for MQW threshold current density is at the first minimum values and then shows a considerable increase with threshold gain, in case the $R_1 = 0.9\ and\ R_2 = 0.7$ will be threshold gain for AlGaAs $g_{th} = 2544 cm^{-1}$ and HgCdTe threshold gain is $g_{th} = 1.02 \times 10^5 cm^{-1}$ for threshold current density $J_{th} = (5784,1327)\, A/cm^2$ respectively.

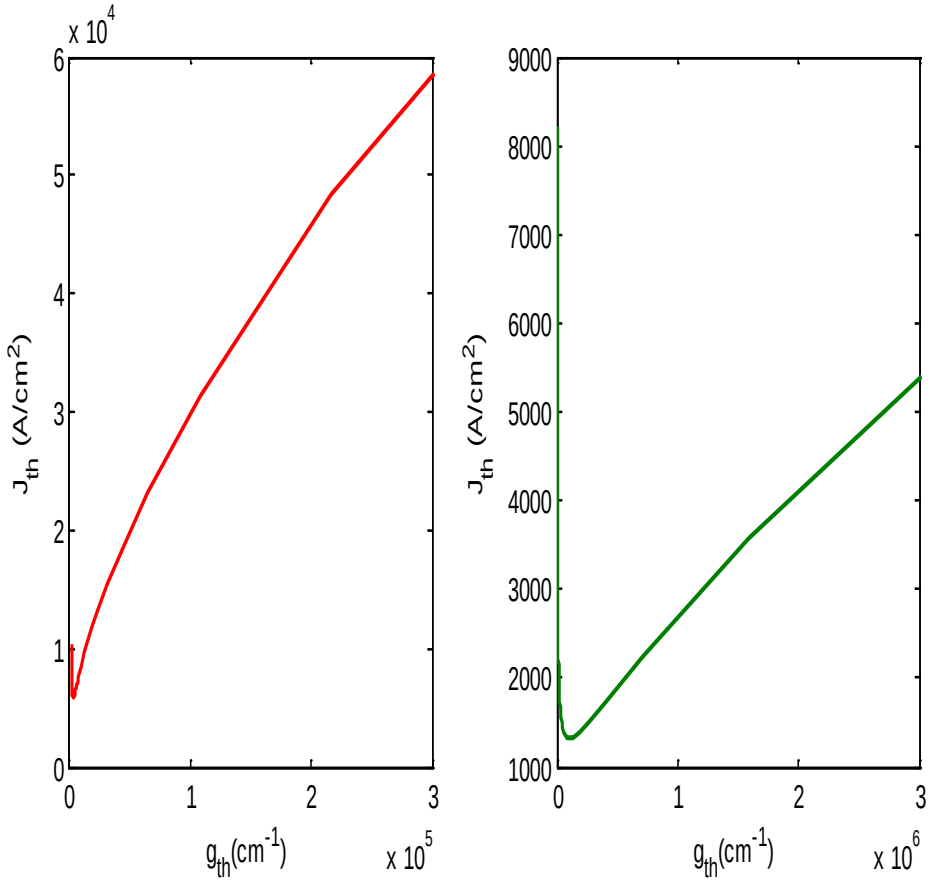

$(a) Al_{0.3}Ga_{0.7}As/GaAs$ $(b) Hg_{0.2}Cd_{0.8}Te/Hg_{0.5}Cd_{0.5}Te$

Fig. (3-14) Threshold current density as a function of threshold gain with barrier width 2nm: (a) $Al_{0.3}Ga_{0.7}As/GaAs$ 3QWs and (b) $Hg_{0.2}Cd_{0.8}Te/Hg_{0.5}Cd_{0.5}Te$ 5QWs

3.6.4 The cavity length

Threshold current density as function of cavity length (L) for facet reflectivity for MQW structure as shown in fig (3-15), we notice the fast reduction with threshold current density to limit (50 cm) after this value threshold current density values are constant with increasing cavity length for two systems MQW $Al_{0.3}Ga_{0.7}As/GaAs$ and $Hg_{0.2}Cd_{0.8}Te/Hg_{0.5}Cd_{0.5}Te$, with two different reflectivity $R_1 = 0.9$ and $R_2 = 0.7$ and $eq.(2-47)$

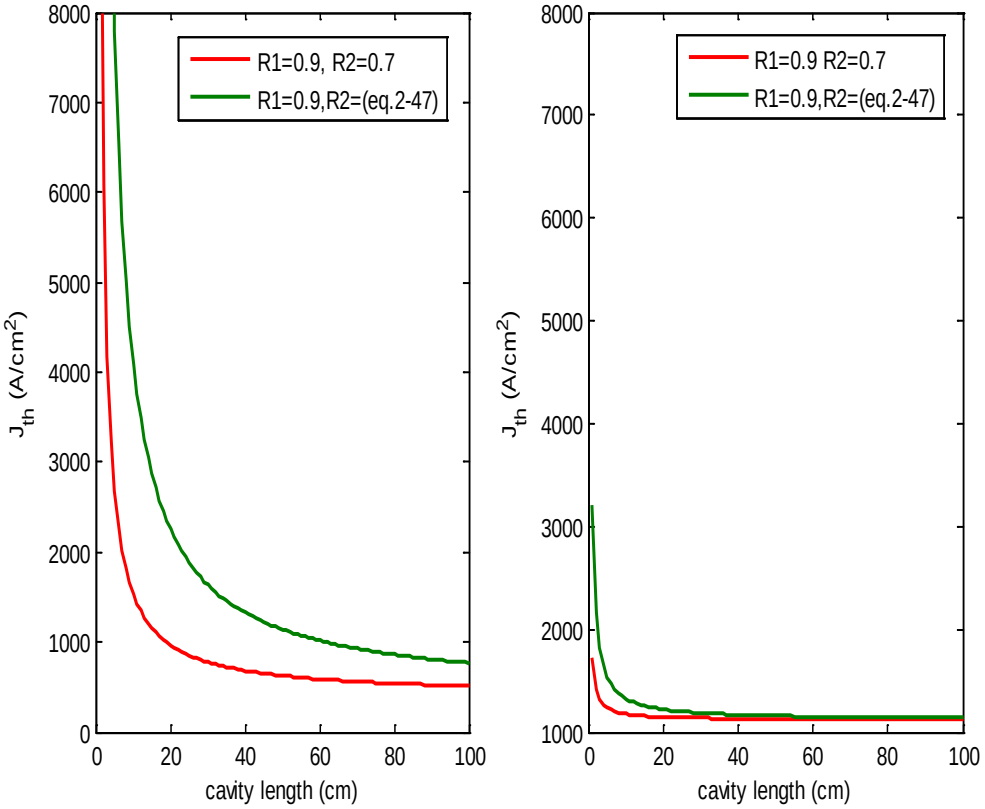

$(a) Al_{0.3}Ga_{0.7}As/GaAs$ $(b) Hg_{0.2}Cd_{0.8}Te/Hg_{0.5}Cd_{0.5}Te$

Fig.(3-15) Threshold current density as a function of cavity length with two different reflectivity for: (a) $Al_{0.3}Ga_{0.7}As/GaAs$ 3QWs and(b) $Hg_{0.2}Cd_{0.8}Te/Hg_{0.5}Cd_{0.5}Te$ 5QWs.

3.7 Output power

The influence of injection current on output power illustrates in fig. (3-16) for multi-quantum well for $Al_{0.3}Ga_{0.7}As/GaAs\ and\ Hg_{0.2}Cd_{0.8}Te\ /Hg_{0.5}Cd_{0.5}Te$ MQW systems. This figure plotted by using eq. (2-59) and (2-64). It's clear that the current increases. When the power is zero the value of current represents the threshold current is approximately I_{th}=11.6mA for$Al_{0.3}Ga_{0.7}As/GaAs$ and$Hg_{0.2}Cd_{0.8}Te\ /Hg_{0.5}Cd_{0.5}Te\ I_{th}$=2.7mA

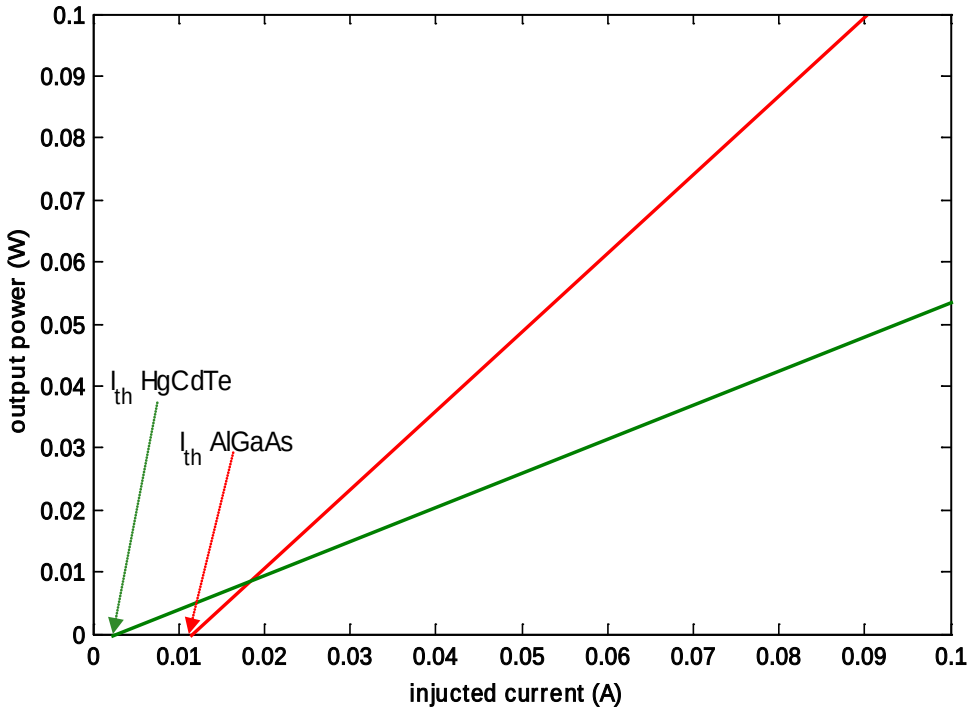

Fig. (3-16) the output power as a function of injected current for $Al_{0.3}Ga_{0.7}As/GaAs$ 3QWs $and\ Hg_{0.2}Cd_{0.8}Te/Hg_{0.5}Cd_{0.5}Te$ 5QWs.

Fig. (3-17) explanation the variation of output power with injection current density for multi quantum well laser ($Al_{0.3}Ga_{0.7}As/GaAs\ and\ Hg_{0.2}Cd_{0.8}Te/Hg_{0.5}Cd_{0.5}Te$) MQW structures at room temperature as the small values of current density less than threshold current density, when the current density is increased and gain developed, stimulated emission is occurred , and output power start to increase with increasing injection current .

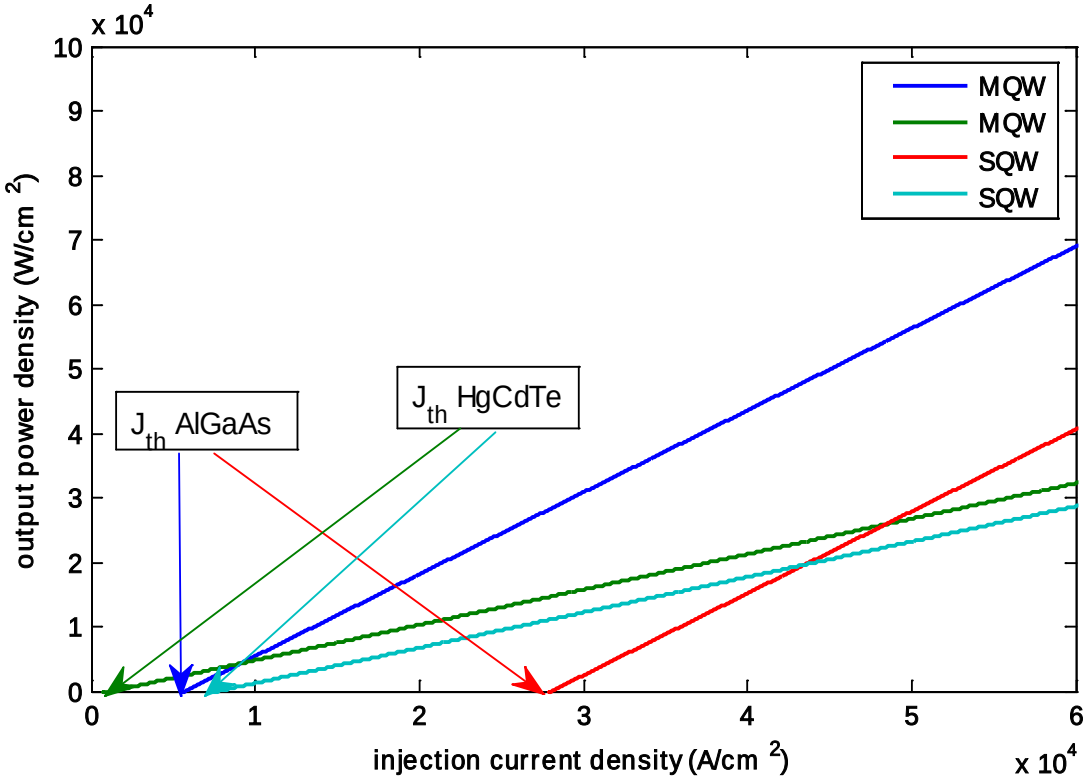

Fig.(3-17) the output power as a function of threshold current density for $Al_{0.3}Ga_{0.7}As/GaAs$ 3QWs and $Hg_{0.2}Cd_{0.8}Te/Hg_{0.5}Cd_{0.5}Te$ 5QWs.

3.8 External Quantum Efficiency

One of the important parameter in laser devices is the efficiency (η).the slop efficiency (η_s) was calculated from figure (3-16) and (3-17) by using eq.(2-59). We noted that $Al_{0.3}Ga_{0.7}As/GaAs$ has η_s higher than $Hg_{0.2}Cd_{0.8}Te/Hg_{0.5}Cd_{0.5}Te$ this result was substituted in eq.(2-58)to calculate external quantum efficiency($\eta_{ext.}$)for both systems we obtained the external quantum efficiency are $\eta_{ext} = 0.89\ and\ \eta_{ext} = 0.97$for $Al_{0.3}Ga_{0.7}As/GaAs$ and $Hg_{0.2}Cd_{0.8}Te/Hg_{0.5}Cd_{0.5}Te$ systems respectively.

We also calculated the external quantum efficiency (η_{ext})by using equation (2-57). The variation of this parameter with cavity length (L) is illustrated in fig.(3-18) we notice that the external efficiency decrease

with increasing the cavity length for $Al_{0.3}Ga_{0.7}As/GaAs$ and $Hg_{0.2}Cd_{0.8}Te/Hg_{0.5}Cd_{0.5}Te$ we for two different refractivity R_2=0.7 and R_2 which calculated from eq.(2-47) where the $\eta_{ext\ AlGaAs} = 0.89$ and $\eta_{ext\ HgCdTe} = 0.97$. We notice that the external quantum efficiency for $Hg_{0.2}Cd_{0.8}Te/Hg_{0.5}Cd_{0.5}Te$ 5QWs higher than η_{ext} for $Al_{0.3}Ga_{0.7}As/GaAs$ 3QWs. Because the deferent in energy gap and internal efficiency where GaAs has E_g very higher than $Hg_{0.5}Cd_{0.5}Te$ and the η_{int} for $Al_{0.3}Ga_{0.7}As/GaAs$ is less than $Hg_{0.2}Cd_{0.8}Te/Hg_{0.5}Cd_{0.5}Te$ which evaluated from reference[50]

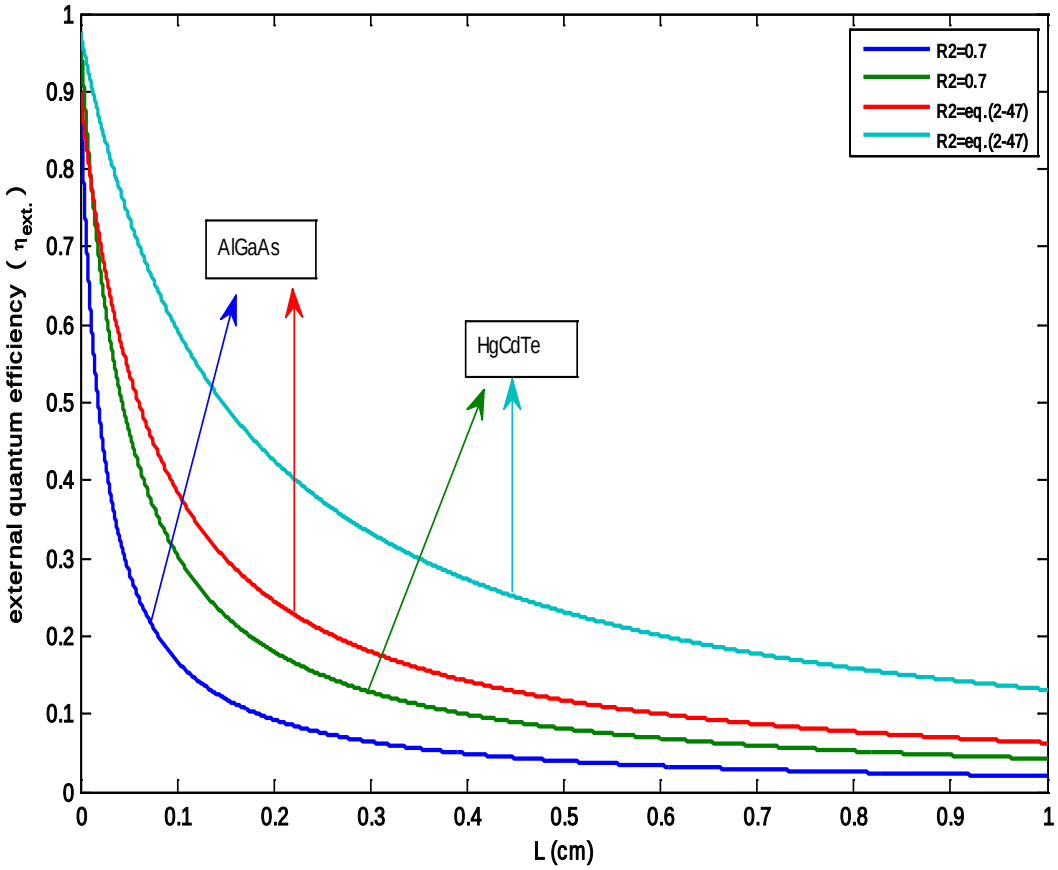

Fig. (3-18) External efficiency as a function of the cavity length for $Al_{0.3}Ga_{0.7}As/GaAs$ 3QWs and $Hg_{0.2}Cd_{0.8}Te/Hg_{0.5}Cd_{0.5}Te$ 5QWs.

CHAPTER FOUR

CONCLUSION AND FUTURE WORK

4.1. Conclusion

In conclusion, $Al_{0.3}Ga_{0.7}As/GaAs$, *and* $Hg_{0.2}Cd_{0.8}Te/Hg_{0.5}Cd_{0.5}Te$ Quantum well laser structures emitted wavelength 872 and 2200nm, respectively in IR range. For two systems, the optical confinement factor of this structure increases with increasing well widths. It has highest (best) value for smallest barrier width (2nm). The best value of the optical confinement factor is occurring at well number 3 for $Al_{0.3}Ga_{0.7}As/GaAs$ but at N_w=5 for $Hg_{0.2}Cd_{0.8}Te/Hg_{0.5}Cd_{0.5}Te$. The optical confinement factor for Single quantum well is very small comparison with multi quantum well for same well and barrier widths. The optical confinement factor of quantum well laser structure for wavelength emitted at inter-sub-band transition is high but with short wavelength in a UV and X-ray.

Through the comparison of the theoretical calculated of laser parameters for $Al_{0.3}Ga_{0.7}As/GaAs$ 3QWs and $Hg_{0.2}Cd_{0.8}Te/Hg_{0.5}Cd_{0.5}Te$ 5QWs as: optical confinement factor, threshold current density, threshold gain, and output power. Demonstrated the optical confinement factor is very important parameter for the performance of these structures.

The optical confinement factor value of $Al_{0.3}Ga_{0.7}As/GaAs$ 3QWs structure is (0.308) by using quantum well width is *W*=21.5nm, and $Hg_{0.2}Cd_{0.8}Te/Hg_{0.5}Cd_{0.5}Te\,5QWs$ is (0.0224) with quantum well width *W*=11.3nm. The barrier width for each systems is B=2nm. That means the optical confinement factor for $Al_{0.3}Ga_{0.7}As/GaAs$ 3QWs higher than $Hg_{0.2}Cd_{0.8}Te/Hg_{0.5}Cd_{0.5}Te$ 5QWs

For the above structures the threshold current density ($J_{th\ AlGaAs} = 5784\ A/cm^2$) is higher than ($J_{th\ HgCdTe} = 1327\ A/cm^2$), threshold gain ($AlGaAs\ g_{th} = 2544cm^{-1}\ and\ HgCdTe\ g_{th} = 1.02\times 10^5$) can be obtained together with efficiency (89%for $Al_{0.3}Ga_{0.7}As/GaAs$ and 97% for $Hg_{0.2}Cd_{0.8}Te/Hg_{0.5}Cd_{0.5}Te$). $Hg_{0.2}Cd_{0.8}Te/Hg_{0.5}Cd_{0.5}Te$).

From the above result, we can use $Hg_{0.2}Cd_{0.8}Te/Hg_{0.5}Cd_{0.5}Te$ as 5QWs laser device.

Table (4-1) optimum result for $Al_{0.3}Ga_{0.7}As/GaAs$ 3QWs and $Hg_{0.2}Cd_{0.8}Te/Hg_{0.5}Cd_{0.5}Te$ 5QWs

Parameter	$Al_{0.3}Ga_{0.7}As/GaAs$	$Hg_{0.2}Cd_{0.8}Te/Hg_{0.5}Cd_{0.5}Te$
Γ	0.308	0.0224
W	21.5nm	11.3nm
J_{th}	5784 A/cm^2	1327 A/cm^2
g_{th}	2544cm^{-1}	1.02× $10^5 cm^{-1}$
$\eta_{ext.}$	89%	97%

4.2. Future Work

The following are the suggestions for future work:

1- Study the optical confinement factor as a function of composition (x) of Al in AlGaAs and of Cd in HgCdTe.
2- Verify Practical for validity of the theoretical results.
3- Used $HgCdTe$ as a quantum wire and quantum dot lasers.
4- Calculated the effective mass of materials for nano-scale structures to used Accuracy account to be used as nanostructures.

REFERENCES

References

[1]A.M. panich "Electronic properties phase transition in low-dimensional semiconductor ", Ben-Gurion University of the Negev, P.O. Box 653 Beer Sheva 84105, Israel e-mail: pan@bgu.ac.il.

[2] O. Bisi,S.U. Campisano,L. Pavesi and F. Priolo "Sillcon Based Microphotonics : from Basics to Application" IOS Press (1999).

[3] F.M.Peeters Brazilian Journal of Physics, Vol.22, No.3, pp: 183-193 (1992).

[4] Clive Emary," Theory of Nanostructures",February 16, (2009).

[5] John M. Senior, Optical Fiber Communications Principles and Practice, 3^d *edition*(2009).

[6] V. V. Apollonov, A. M. Prokhorov, and A. H. Guenther, "Power optics, problems, developments, and opportunities", laser physics, Vol. 11, No. 7, pp. 1-4 (2001).

[7] J. Garcia. Ojalvo, J. Casademont, M. C. Torrent, C. R. Mirasso, and J. M. Sancho, "Coherence and synchronization in diode-laser arrays with delayed global coupling", International Journal of Bifurcation and Chaos, Vol. 9, No. 11, pp. 2225-9 (1999).

[8]Dan Alexandru Anghel," Modeling Quantum Well Lasers", University "Politehnica" of Bucharest, 28 November (2011)

[9] P. Harrisona) and R. W. Kelsall**,**" Population inversion in optically pumped asymmetric quantum well terahertz lasers", University of Leeds, Leeds LS2 9JT, United Kingdom, 17 February (1997).

[10] S.M. SZE, Physics of Semiconductor Device, 3^dedition (2007).

[11]Ting Hao," Calculation and Experimental Verification of Longitudinal Spatial Hole Burning in High-Power Semiconductor Lasers",Rose-Hulman Institute of Technology, May (2014).

[12] P. Bhattacharya, Semiconductor_Optoelectronic_Devices, 2nd edition Pearson Education, Inc, (2002).

[13] Thomas L. Floyd, "Electronic Devices", 7^dedition (2009).

[14]Donald A.Neanen,"Semiconductor Physics and Devices basic principles", university of New Mexico, 3^dedition (2003).

[15]G. D. Mahan,and H. B. Lyon, "Thermoelectric devices using semiconductor quantum wells", J. Appl. Phys., Vol. 76, No. 3, pp. 1899-901 (1994).

[16] S. O. Kasap, Optoelectronics and Photonics, Prentice Hall International, NJ, USA, (1999).

[17] J.Hill,"Laser Diode Technology and Applications", Portland State University,Physics 464, (2005).

[18] M. Arnold, "Characterization of linewidth Enhancement Factor for InGaAsP and InGaAlAs Quantum wells", university of Surrey,Dec (2010).

[19] David A. B. Miller," Optical Physics of Quantum Wells", Rm. 4B-401,At &T Bell Laboratoties, USA.

[20] David Sands, Diode Lasers, University of Hull, UK, (2005).

[21] Peter S. Zory, "Quantum Well Lasers", Academic Press, pp. 1-13, (1993).

[22] J. P. Colinge, Physics of semiconductor Devices, University of California, Springer (2005).

[23] Matthias Pospiech, Sha Liu,"laser Diodes an Introduction", University of Hannover, Germany, May (2004).

[24] R. Hamad Abdallah, Msc. thesis "Theoretical Analysis for the cooling of laser diode package by using Peltier Effect", university of Baghdad, College of Education, Ibn AL-Haitham, April,(2008).

[25] Pamela L. D.,Luis F. Chi Sh., Hand Book Of Optics :Chapter 19, Vol.II 3^dedition , Washington,(2011)

[26]M. Jaros, Physics and Applications of Semiconductor Microstructures, Clorendon Press-Oxford, (1989).

[27] Norton, P. "HgCdTe infrared detectors, Opto-Electronics Rev. Vol. 10, No. 3, pp.159–74 (2002).

[28] Anne M. Itsuno "Bandgap-Engineered HgCdTe Infrared Detector Structures for Reduced Cooling Requirements", University of Michigan (2012).

[29] Yakushev, M. V."HgCdTe nanostructures on GaAs and Si substrate for IR and THz radiation detecting", Journal of Physics: Conference Series 345, pp.1-15 et al.(2012).

[30] Pierre-Yves Emelie "HgCdTe Auger-Suppressed Infrared Detectors Under Non-Equilibrium Operation"The University of Michigan (2009).

[31] D. G. Seiler, J. R. Lowney, C. L. Littler, and M. R. Loloee, "Temperature and composition dependence of the energy gap of $Hg_{1-x}Cd_xTe$ by two- photon magnetoabsorption techniques", J. Vac. Sci. Technol. A 8, No. 2, pp.1237-44 (1989).

[32] B. Jensen and A. Torabi, "Linear and nonlinear intensity dependent refractive index of $Hg_{1-x}Cd_xTe$", J. Appl. Phys., Vol. 54, No.10, pp. 5945-9(1983).

[33] R. Dingle and C. H. Henry, “Quantum Effects in Heterostructure Lasers,” U.S. Patent 3 982 207, Sept. 21,(1976).

[34] Levon V. Asryan, Serge Luryi,"Internal Efficient of semiconductor Lasers With a Quantum-Confined Active Region", IEEE Journal of Quantum Electronics, Vol.39, No.3, March (2003).

[35]Michal Grochol,"Optical Properties of Semiconductor Nanostructures in Magnetic Field"Universität zu Berlin,15 January (2007)

[36] C. Kittle "Introduction to Solid State Physics"8^{th}edition, John Wiley & Sons (2004).

[37] J. M. Martinez-Duart,R. J. Martin-Palma and F. Agullo-Rueda," Nanotechnology For microelectronics and Optoelectronics", Elesvier B.V., AE Amsterdam, The Netherlands (2006).

[38] F.Charra and S. Gota-Goldmann,"Mesoscopic and Nanostructured Materials"part5, Springer Berlin Heidelberg (2005).

[39] G.Schmid, M. Decker,H. Fuchs, and W. Grunwtso"Small Dimensions and Material Properties A Definition of Nanotechnology "Europaische Akadamic, November (2003).

[40] A.Irrera, ph.D. Thesis," Light Emitting Devices based on Silicon Nanostructure " University Degli Studi Di Catania (2003).

[41] Samuel S. Mao," Nanolasers: Lasing from nanoscale quantum wires", Int. J. of Nanotechnology, Vol. 1, Nos. 1/2, (2004).

[42]Britteny Spears'Guide to Semiconductor physics http:// brineyspears.ac/physics/dos/dos. htm.

[43] Huzan Tanksalwalla,"Semiconductor quantum well and quantum wire lasers", San Jose State University, (1991).

[44] Haji Awang Makarimi Haji Awang Kasim," Threshold Current Temperature Dependence of Indium Phosphide Quantum Dot Lasers", Cardiff University, November (2014).

[45] Liboff RL, Introductory Quantum Mechanics,4^{th} end. Addison-Wesley, San Francisco, (2003): http//www.garlandscience. com/res/ pdf/9780815344247_ch09.pdf

[46]Omar Manasreh,"Semiconductor Heterojunctions and Nanostructures", University of Arkansas Fayetteville, Arkansas, (2005).

[47] Li Jiang, "Theoretical Study of Performance Characteristics of Semiconductor Quantum Dot Lasers", September 2, (2008).

[48] P. J. A. Thijs and T. Dongen, Ext. Abs. 22nd Int. Conf. Solid State Devices and Materials, Sendai, Japan (1990).

[49] Y.Arakawa, A.Yariv, "Quantum well laser-Gain spectra Dynamics", IEEE Journal of Quantum Electronics, Vol.QE-22, No.9, sep. (1986).

[50] Y.Jiang M. C. Teich,W. I. Wang, "Carrier lifetime and threshold current in HgCdTe double heterostructure quantum –well lasers", Columbia university ,New York, January (1991).

[51] A. S.P. and Georgy G. Zegrya, "Auger recombination in Semiconductor Quantum well", Technical Institute Russia, Dec. (1998).

[52] Alex T. H. and E. Herbert Li.,"waveguiding in vertical cavity Quantum –well structure Defined by Ion Implantation", Journal of Lightwave Technology, Vol, 16, No. 8, August (1998).

[53]Manish Jain, "An investigation of broad gain spectrum InGaAs/InAlGaAs quantum well lasers latticed matched to InP", The University of Glasgow, September (2002).

[54] A.Stintz.P.G., and K. J. Malloy " Comparison of the carrier induced refractive index, gain, and linewidth enhancement factor in quantum dot and quantum well lasers", Applied Physics,Vol 84,No 7, 16 February (2004).

[55] Nelson Tansu and L. J. Mawst, "Current injection efficiency of InGaAsN quantum-well lasers" Journal of Applied Physics 97, 9 February (2005).

[56] Jonathan M. B., "Near Infrared Optical Manipulation of a GaAs/AlGaAs Quantum Well in the Quantum Hall Regime", McGill University Montr´eal, Qu´ebec, Canada,August (2008).

[57] H. Zaho. R. A. Arif.Y.-K," Optical gain analysis of strain-compensated InGaN–AlGaN quantum well active regions for lasers emitting at 420–500nm", Opt Quant Electron, 9 January (2008).

[58] S. A. Sayid, Cannard,Xain Chen,S.J.sweeney,"Thermal Performance of 1.55μm InGaAlAs Quantum Well Buried Heterostructure Lasers" University of Surrey, Guildford, GU2 7XH, UK, April (2010).

[59] A. Asgari, S. Dashti,"Optimization of optical gain in $Al_xGa_{1-x}N/GaN/Al_xGa_{1-x}N$ Strained quantum well laser", Applied Physics, University of Tabriz, Tabriz 51665-163, Iran, 17 August (2011).

[60] J. W. Ferguson, P. B. and P. M. Smowton ,"Optical Gain in GaInNAs and GaInNAsSb Quantum Wells", IEEE Journal of Quantum Electronics, Vol. 47, No. 6,Juneuary (2011).

[61] Michael Wootten," Superluminescence diodes at 2.4 microns from GaInAsSb/AlGaAsSb quantum well heterostructures for optical glucose sensing", University of Iowa, May (2013).

[62] Tawsif Ibne Alam, Md. Abdur Rahim and Rinku Basak," Effects of Variation of Quantum Well Number on the Performance of a Designed 635nm $Ga_{0.5}In_{0.5}$P/ $(Al_{0.7}Ga_{0.3})_{0.5}In_{0.5}$P Multiple Quantum Well Red Laser", International Journal of Multidisciplinary Sciences and Engineering, Vol. 4, No. 2, February (2013).

[63] V. Mitin, D. Sementsov and N. Vagidov "Quantum Mechanics for Nanostructures", University at Buffalo, The State University of New York, (2010).

[64] T. Numai, "Fundamental of Semiconductor Lasers", 2^d edition Springer Series in optical Sciences 93, (2015).

[65] Martina De Laurentis and Andrea Irace, "Optical Measurement Techniques of Recombination Lifetime Based on the Free Carriers Absorption Effect", Journal of Solid State Physics, 24 June (2014).

[66] Barnbas Achakpa Ikyo, " Electron-Hole and Photon Recombination Processes in Quantum Well Semiconductor Lasers", American Journal of Optics and Photonics, Vol. 3, No. 5, pp. 80-84, (2015).

[67] David J. Klotzkin, Introduction to Semiconductor Lasers for Optical Communications-An Applied Approach, Springer-verlag New York, (2014).

[68] H.Kressel,"Material for Hetrojunction Devices", Ann.Rev. Mater Sci., Vol. 10, pp. 287-309, (1980).

[69] A. Kasukawa, et al., "Recent Progress of High Power Semiconductor lasers", Furukawa Rev. No. 19, (2000).

[70]Chukwuocha, E. O. et al. (2012). Theoretical Studies on the Effect of Confinement on Quantum Dots Using the Brus Equation. World Journal of Condensed Matter Physics, 2, 96-100.

[71] Safa Kasap ,Peter Capperbook: Springer Handbook of Electronic and Photonic Materials, pp.1021-1040**,** (2007).

[72] Shiang-Feng Tang, Tzu-Chiang Chen, Shih-Yen Lin and Hsing-Yuan Tu," Intersubband Transitions in the Quantum Dot Layers for Quantum Confined Photodetector", Academia Sinica National Taiwan UniversityTaiwan, R.O.C., (2010)

[73] M.Zalizny ," intersubband transitions in n-type quantum well system", Opto-Electronics Review 7(2), 81-86 (1999).

[74] Saman Q. Mawlud," Bias-Voltage Dependence on Thermoelectricn Cooler Coefficient for Al0.7Ga0.3As and In0.2Ga0.8As SQW Laser Diode", Salahaddin Univ.Erbil, Kurdistan Region, Iraq (2010).

[75] Nipu R. Barai, Rinku Basak, " Performance Analysis of SMQW SOA Based On Optical Confinement Factor", American International University-Bangladesh, August (2014).

[76] M.F.Khodr, P. J. McCann,and B. A. Mason,"Optimizing and Engineering EuSe-Pb$Se_{0.78}Te_{0.22} - EuSe$ Multiple –Quantum-Well Laser Structures", IEEE Journal of Quantum Electronics,Vol.34,No.9. September (1998).

[77] Alhuda A. Al-mfrji, "Saturation Gain Characteristics of Quantum Well Semiconductor Optical Amplifier", Nahrain University, College of Engineering Journal (NUCEJ) Vol.14 No.2, pp.205-212, (2011).

[78] Majed Khodr "Modeling PbSe/PbSr/Se Quantum well Lasers for Breath Analysis Applications", American University of Ras Al Khaimah, (2015).

[79] Gerd Keiser," optical Fiber Communication", 3^dedition (2000).

[80] J. Piprek," Semiconductor Optoelectronic Devices: Introduction to Physics and Simulation"University of California at Santa Barbara, (2003).

[81] Mohammed Abdul Majid,"GaAs-Based Quantum Dot Emitters for Telecomms and Broadband Application, University of Sheffield, August (2011).

[82] Y. Arakawa, and H. Sakai, "Multidimensional quantum well laser and temperature dependence of its threshold current', Appl. Phys Lett., 1982, 40, (11), pp.939-941.

[83] ELI KAPON," Quantum Wire Lasers", IEEE. Vol.80, No.3, March (1992).

[84] Kamran S. Mobarhan,"Test and characterization of laser diode determination of principal parameters, University California

[85] H. Zaho,G.. Liu,J.Zhang . R. A. Arif.Y.-K and N. T.," Analysis of Internal Quantum Efficiency and Current Injection Efficiency in III-Nitride Light-Emitting Diodes", Journal of Display Technology, Vol. 9, No. 4, April (2013).

[86] Raja Rashidul Hasan and Rinku Basak," Characteristics of a Designed 1550 nm AlGaInAs/InP MQW VCSEL", International Jouurnal of multidiscipline Sciences and Engineering, Vol. 4, No. 1, January (2013) .

[87] Irina Stateikina," Optoelectronic Semiconductor Devices - Principals and Characteristics", Concordia University (2002).

[88] Vorgelegt von "Realization of High Power Diode Lasers with Extremely Narrow Vertical Divergence" (2011).

[89] O. Svlto, Principles of laser, plenum Press-New York, 3^dedition, (1989)

[90] ARogalskl," HgCdTe infrared detector material: history, status and outlook″ Institute of Applied Physics, Military University of Technology, 22 August 2005.

Appendix

MATLAB Program for Calculating as Function of Well Width for Single Quantum Well and Multi-Quantum Well

Function Figure (3-6)

****************************Constants*********************

```
W=0:0.1:30; Well width (nm)
T=300  Room temperature(K)
B=2; barrier width (nm)

For AlGaAs
Xw=0; well composition
Xb=0.3; barrier composition
Xc=1; cladding composition
Nw=3; number of well
Nb=Nw-1; barrier of well
γw=3.59-0.62*Xw;
γb=γw -0.62*Xb;
γc=γw-0.62*Xc;
Eg=1.424+1.247*Xw;
λ=872;

For HgCdTe
Nw1=5;Nb1=Nw1-1;
Xw1=0.5;Xb1=0.8;Xc1=0.9;
γw1=4.427-3.617*Xw1+2.055*Xw1^2;
γb1=4.427-3.617*Xb1+2.055*Xb1^2;
γc1=4.427-3.617*Xc1+2.055*Xc1^2;
Eg1=-0.302+1.93*Xw1-
0.81*(Xw1)^2+0.832*(Xw1)^3+(5.35*(1-2*Xw1)*10^-4*((-
1822+T^2)/(255.2+T^2)))
λ1=2200;
```

**********Equation**********

```
d=(Nw*W)+(Nb*B);
γr=((Nw*W*γw)+(Nb*B*γb))./d;
C1=((2*pi)/λ)*W*sqrt((γw)^2-(γb)^2);
C'=2*pi*(d./λ).*sqrt(γr.^2-γc^2);
Gama1=C1.^2./(C1.^2+2);
Gama=C'.^2./(C'.^2+2);
Gamam=Gama.*((Nw*W)./d);
d1=(Nw1*W)+(Nb1*B);
γr1=((Nw1*W*γw1)+(Nb1*B*γb1))./d1;
C1H=((2*pi)/λ1)*W*sqrt((γr1)^2-(γb1)^2);
C'H=2*pi*(d1./λ1).*sqrt(nr1.^2-γc1^2);
Gama1H=C1H.^2./(C1H.^2+2);
GamaH=C'H.^2./(C'H.^2+2);
GamamH=GamaH.*((Nw1*W)./d1);
subplot(1,2,1)
plot(W,Gama1,W,Gamam);
xlabel('Well width (nm)')
ylabel('confinement Factor ( \Gamma )')
text(21,0.316,'MQW')
text(22,0.04,'SQW')

subplot(1,2,2)
plot(W,Gama1H,W,GamamH);
xlabel('Well width (nm)')
ylabel('confinement Factor ( \Gamma )')
text(21,0.027,'MQW')
text(21,0.0044,'SQW')
```

الخلاصـــة

هذا البحث يصف مقارنة نظرية بين نظامي $Al_{0.3}Ga_{0.7}As/GaAs$ و $Hg_{0.2}Cd_{0.8}Te/Hg_{0.5}Cd_{0.5}Te$ لليزر البئر الكمي ذو التركيب غير المتجانس. حيث تم دراسة تأثير العوا مل المختلفة لهذا التركيب مثل عرض البئر وعرض الحاجز للبئر الكمي المفرد والمتعدد على عوامل الليزرمثل عامل التقيد البصري وتيار العتبة وكثافة تيار العتبة والربح البصري وقدرة الخرج والكفاءة . بالاضافة الى دراسة كثافة الحالات للبئر الكمي.

افضل قيمة لعامل التقييد البصري (0.308) للتركيب $Al_{0.3}Ga_{0.7}As/GaAs$ ذو ثلاثة ابار كمية و (W=21.5nm) و (0.0224) للتركيب $Hg_{0.2}Cd_{0.8}Te/Hg_{0.5}Cd_{0.5}Te$ ذو خمسة ابار كمية و (W=11.3nm). عامل التقيد له تحسن كبير في التركيب المتعدد الابار افضل من التركيب ذو البئر الكمي المفرد . وأظهرت النتائج ان عامل التقييد للتركيب المتعدد الابار اكبر منه للبئر الكمي المنفرد بمقدار 18 مرة للتركيب $Al_{0.3}Ga_{0.7}As/GaAs$ وبمقدار 25 مرة للتركيب $Hg_{0.2}Cd_{0.8}Te/Hg_{0.5}Cd_{0.5}Te$.

هذا التحقيق لتحسين عمل نبيطة الليزر دايود من خلال تأثير عامل التقييد البصري على الربح وتيار العتبة والقدرة الخارجة والكفاءة تحت الانحياز الامامي في المنطقه الفعالة، كانت كثافة تيار العتبة

$J_{th\,AlGaAs} = 5784 A/cm^2$ و $J_{th\,HgCdTe} = 1327\ A/cm^2$

وكفاءة (89% لـ $Al_{0.3}Ga_{0.7}As/GaAs$ و 97% لـ $Hg_{0.2}Cd_{0.8}Te/Hg_{0.5}Cd_{0.5}Te$)

جمهورية العراق
وزارة التعليم العالي والبحث العلمي
جامعة بغداد
كلية التربية للعلوم الصرفة / أبن الهيثم

مقارنة نظرية بين HgCdTe و AlGaAs لنظامي البئر الكمي الليزري ذو التركيبين غير المتجانسين

رسالة مقدمة الى

مجلس كلية التربية للعلوم الصرفة-ابن الهيثم، جامعة بغداد

كجزء من متطلبات نيل شهادة ماجستيرعلوم في الفيزياء

من قبل

وديان كاظم عبد الزبيدي

بكالوريوس فيزياء/جامعة بغداد/2013

بأشراف

د. ابتسام محمد تقي سلمان

1437هـ 2016 م